WATER ADSORPTION, MICROSTRUCTURE, AND VOLUME CHANGE BEHAVIOR OF CLAY MINERALS AND SOIL

by

John Charles Parker

Dissertation submitted to the Graduate Faculty of the
Virginia Polytechnic Institute and State University
in partial fulfillment of the requirements
for the degree of

DOCTOR OF PHILOSOPHY

in

Agronomy

APPROVED:

D. F. Amos, Co-Chairman

L. W. Zelazny, Co-Chairman

T. B. Hutcheson, Jr.

R. D. Krebs

J. P. Wightman

August 1980

Blacksburg, Virginia

ACKNOWLEDGEMENTS

Many thanks are due Dan F. Amos and Lucian W. Zelazny who, in addition to offering encouragement and friendship, served as willing co-conspirators and co-chairmen of my graduate committee.

Thanks also to T. B. Hutcheson, J. P. Wightman, D. A. Lietzke and R. D. Krebs for serving on the committee.

Thanks are extended to who typed the manuscript, to who helped draft figures and to , , and who helped with various aspects of the field and laboratory work.

Finally, special thanks to and and for spiritual succor.

TABLE OF CONTENTS

LIST OF TABLES

LIST OF FIGURES

Page

INTRODUCTION

Shrinking and swelling accompanying changes in moisture content commonly occur in soils with appreciable clay content. However, the magnitude of these volume changes varies over a broad continuum. In moderation, shrinking and swelling may contribute to the formation of soil aggregates which improve conditions for plant growth. When volume changes are large, however, unique problems are posed to human enterprises.

In extreme cases, tension cracks, which form on drying, may present hazardous footing for livestock. When these cracks swell shut upon wetting, hydraulic conductivity becomes very low, as does gaseous diffusivity, restricting the growth of most crops. Seedling emergence and root growth may be physically restricted and roots may be severed as shrinking and swelling procedes.

Such soils also pose problems to engineering ventures. Highways, buildings, pipelines and utility lines may be severely damaged by differential earth movements if special design precautions are not taken. Disposal of liquid wastes is not feasible on highly expansive soils because of their low hydraulic conductivity.

Much effort has been expended by researchers to learn how to deal with expansive soils and to understand the mechanisms which control these volume changes. However, no concensus has been reached regarding the fundamental physical processes involved in soil volume changes associated with water adsorption. The purpose of this study was to investigate and elucidate the mechanisms of water adsorption and

swelling by expansive clay minerals and to determine how they are affected by differences in microstructure.

The study consists of three experiments. The first investigates the mechanisms of water adsorption and swelling of Ca-montmorillonite and evaluates the effects of compaction on clay microstructure and on the relative contributions of various mechanisms of water adsorption and swelling to total adsorption and volume change. The purpose of the second experiment was to investigate the effects of cation saturation on the relative contributions of inter- and intra-crystalline water adsorption to total adsorption and swelling, to evaluate the significance of osmotic adsorption to intercrystalline expansion, and to study the effects of micromorphology on swelling by montmorillonite and vermiculite. The third experiment considers the effects of compaction and cyclic wetting and drying on the volume change behavior of two soils.

MECHANISMS OF WATER ADSORPTION, SWELLING AND SHRINKING: AN INTERPRETIVE REVIEW

Soil volume changes are manifestations of unbalanced forces within a soil mass. These unbalanced forces may arise from changes in geostatic or applied forces or from changes in forces of a physico-chemical nature. In this treatise, only the latter will be considered; however, it should be kept in mind that in nature all of these forces act together (McDowell, 1956; Rhoades et al., 1969; Talsma, 1977; Dakshanamurthy, 1979) and are separable in concept only. Since shrinking and swelling are commonly observed to accompany drying and wetting, it would appear that an understanding of the mechanisms of water adsorption is requisite to an analysis of the physico-chemical forces governing soil volume changes.

Mechanisms of Water Adsorption

Water vapor sorption isotherms of soils and clays generally conform to Type II behavior (Figure 1), characteristic of multilayer adsorption on substances exhibiting broad pore size distributions (Gregg and Sing, 1967). Adsorption of the first one or two monolayers at low relative pressures is strongly influenced by H_2O-surface and H_2O-exchangeable ion interactions. That these attractions are greater than H_2O-H_2O interactions is evidenced by the initially convex shape of the adsorption isotherms (Sposito and Babcock, 1966). At greater distances from the surface, H_2O-H_2O interactions and entropic factors increasingly dominate adsorption.

Water-surface interactions

Interactions between water molecules and mineral surfaces may arise from van der Waals attractions and water-charge site interactions. Three types of van der Waals forces may be distinguished--London dispersion, Debye induction and Keesom orientation. London dispersion forces are the quantum mechanical result of coupled oscillations of electrons in adjacent molecules which may or may not have permanent dipoles. Debye forces arise when the electric field associated with a permanent dipole induces a dipole in an adjacent molecule. Keesom forces develop from the interaction of two polar molecules. Hydrogen bonds, which are a particularly strong type of Keesom orientation due to the relatively high dipole moment of -OH and similar groups, may contribute to water adsorption on mineral surfaces when, for example, the positive dipole of a water molecule orients toward the negative dipole of an SiO_2 surface.

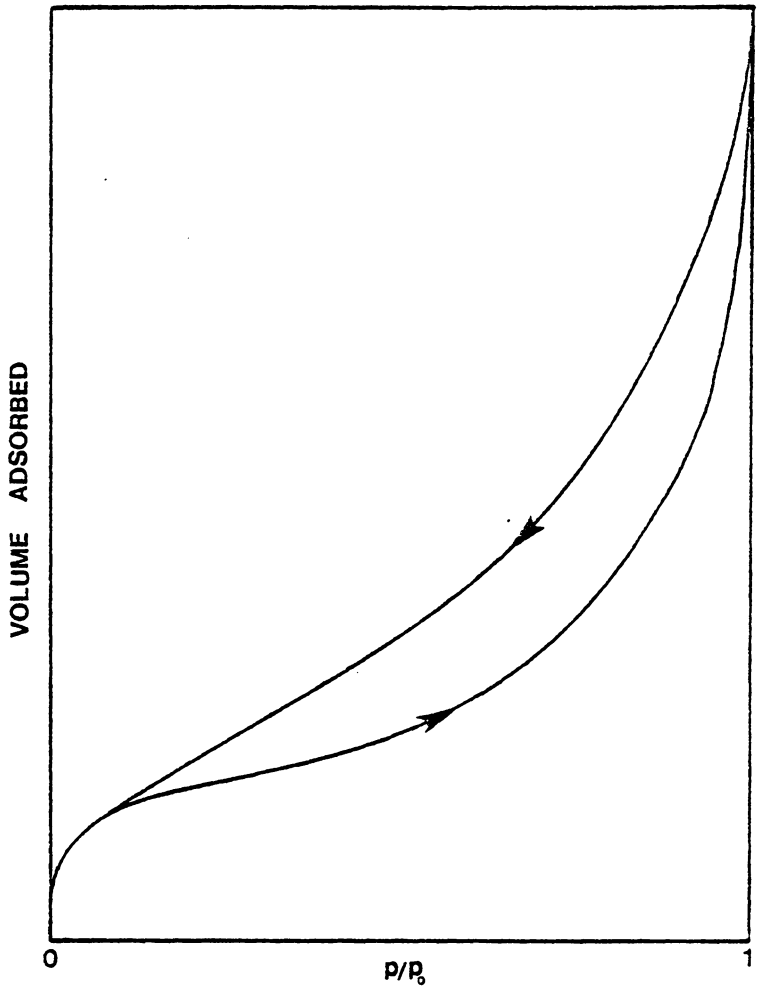

Figure 1. Type II adsorption isotherm with hysteresis typical of water vapor adsorption by soils and clays.

Interaction energies between two single molecules caused by van der Waals attraction are given by:

$$E_{London} = -\frac{3}{2}\,\frac{I_1 I_2}{I_1+I_2}\,\frac{\alpha_1\alpha_2}{x^6} \qquad [1]$$

$$E_{Debye} = \frac{\alpha_1\mu_2^{\,2} + \alpha_2\mu_1^{\,2}}{4\pi\varepsilon x^6} \qquad [2]$$

$$E_{Keesom} = -\frac{2}{3}\,\frac{\mu_1^{\,2}\mu_2^{\,2}}{(4\pi\varepsilon)^2 kTx^6} \qquad [3]$$

where I is the ionization energy, α is the polarizability, μ is the dipole moment, ε is the permittivity, kT is the thermal energy, x is separation distance, and the subscripts 1 and 2 refer to the two molecules under consideration (Hiemenz, 1977). In every case, interaction energies decrease with the sixth power of separation distance. Interaction of a single molecule (e.g., water) with a planar surface (e.g., a phyllosilicate), however, is considerably stronger than between two single molecules due to the greater number of bond pairs, and will exhibit a negative third power distance dependency (Adamson, 1976).

Most mineral surfaces exhibit charge development due to crystal substitutions, ionization of functional groups or adsorption of potential determining ions. These charge sites are subject to hydration in a manner analogous to the hydration of ions in solution--by suitable orientation of water dipoles at the charge sites. The interaction energy between a dipole and an ion is given by:

$$E_{\text{ion-dipole}} = -\frac{ve\mu \cos \theta}{4\pi\varepsilon x^2} \qquad [4]$$

where v is the ionic valence, e is the electronic charge, μ the dipole moment, θ is the angle between the ion and dipole field vectors, ε is the permittivity, and x is again the separation distance (Hiemenz, 1977). A contribution to the interaction energy will also be made by ion-induced dipole interactions (Sposito and Babcock, 1966) which are given by:

$$E_{\text{ion-induced dipole}} = -\frac{v^2e^2\alpha}{8\pi\varepsilon x^4} \qquad [5]$$

where α is the polarizability.

The separation distance in Equations 4 and 5 will be affected, especially for the first layer of water, by the surface charge location. For example, a tetrahedral charge site in a 2:1 phyllosilicate would exhibit a shorter separation distance and thus a greater hydration energy than an octahedral charge site. It should be realized, however, that surface charge due to crystal substitutions is likely to be diffused over several surface atoms in which case Equations 4 and 5 may not be strictly valid. Eberl (1980) has

considered the case in which surface charge is taken to be evenly dispersed over a planar surface.

According to Bartell and Suggitt (1954), heat of wetting is a measure of the enthalpy of water adsorption. From measurements on amorphous silica powders, Ihler (1955) determined that the heat of wetting of a pure SiO_2 surface is -130 ergs/cm^2 (following the sign convention that (-) enthalpies are exothermic and (-) free energies spontaneous). Taking the area occupied by a water molecule as 6.25 Å^2 gives an energy of -8.12×10^{-14} ergs/H_2O molecule. This value may be compared to the van der Waals attraction between water molecules separated by 5 Å calculated from Equations 1 to 3 which is -1.41×10^{-14} ergs/molecule at 25°C. Kittrick (1969b) estimated charge site hydration energies by assuming that they behaved similarly to Cl^- ions in bulk solution. Based on the hydration energy of Cl^- of -6.25×10^{-12} erg/ion, and assuming a surface charge of 0.90 meq/g and a surface area of 800 m^2/g (charge density = 3.24×10^4 esu/cm^2) for a typical montmorillonite, we find a charge site hydration energy of -424 erg/cm^2. Comparison with the hydration energy for an uncharged SiO_2 surface of -130 erg/cm^2 shows surface charge to be of great importance to water adsorption.

Water-exchangeable ion interactions

Charges associated with mineral surfaces are balanced by adsorbed ions which may become hydrated in the same manner as surface charge sites. As indicated by Equations 4 and 5, ion hydration energies will increase as ion valence increases and ion size decreases. Accordingly, hydration energies for some cations common in soils range as follows:

Ion hydration energies (10^{-12} erg/ion)

Mg^{++}	Ca^{++}	Na^{+}	K^{+}
-32.0	-27.5	-6.75	-5.35

For a surface charge density of 3.24×10^4 esu/cm^2 typical of a montmorillonite, the contributions of these ion hydration energies to the clay hydration energy are -1079, -931, -457, and -362 erg/cm^2, respectively.

Net surface hydration energy does not necessarily increase with ion hydration energy, however, since ion hydration energies are countered by Coulombic ion-charge site attractions. Coulombic interaction energy between two point charges is given by:

$$E_{Coulombic} = \frac{v_1 v_2 e^2}{4\pi\varepsilon x} \qquad [6]$$

Shainberg and Kemper (1966) have estimated net adsorbed ion hydration energies as the difference between Coulombic surface-ion energies and ion-dipole hydration energies. More refined analyses have been made by Sposito and Babcock (1966) and Kittrick (1969b).

Water-water interactions

Beyond the first layer of adsorbed water, water-water interactions govern continued adsorption to an increasing extent as water-surface and water-exchangeable ion interaction energies diminish as a power function. The dominant mechanism of water-water interaction is H-bonding. It has been calculated that 84.8% of the attractive energy between water molecules is due to Keesom orientation, 4.5% to Debye induction, and 10.5% to London dispersion forces (Hiemenz, 1977).

The unsymetrical forces acting on water molecules at phase boundaries give rise to the phenomena of surface tension. A manifestation of this phenomena is the tendency for systems containing air-water interfaces to minimize their interfacial area. Thus, in porous systems such as soils, water vapor will spontaneously condense in pores to reduce the area of air-water interface. Capillary condensation occurs in increasingly larger pores as the free energy of water vapor (ψ_w) in equilibrium with the liquid phase decreases according to the relation:

$$\psi_w = \frac{2\bar{V}\gamma \cos \theta}{r} \qquad [7]$$

in which $\bar{V}$ is the molar volume of water, γ is the surface tension, θ is the contact angle, and r is the pore size (the radius of a cylindrical pore or the plate separation of a slit shaped pore). Considering water to behave as an ideal vapor yields the Kelvin equation:

$$\frac{2\bar{V}\gamma \cos \theta}{r} = -RT \ln p/p_o \qquad [8]$$

where R is the gas constant, T the absolute temperature, and p/p_o the relative vapor pressure. Equation 8 explains, in part, the exponential increase in water adsorption at high relative pressures (Gregg and Sing, 1967) common to water vapor adsorption (Figure 1).

Entropy effects

Predictions of water adsorption must take into account the contribution of entropy changes to the total free energy change. The hydration of ions in bulk solution may be accompanied by an increase or decrease in entropy depending on the ion's effect on water structure.

Ca^{++} and to a lesser extent Na^{+} and K^{+} decrease the entropy of water, while, for example, Cs^{+} and Rb^{+} cause an increase (Kijne, 1969). As an order of magnitude estimate of the contributions of ion hydration entropy to clay hydration, consider a montmorillonite saturated with Na^{+} ions which undergo an entropy change (ΔS) during hydration in bulk solution of -20 cal deg^{-1}mole $ions^{-1}$ (Hunt, 1965). If the same ΔS occurred for hydration of adsorbed Na^{+}, the entropy contribution to the free energy change $-T\Delta S$ would be only about +28 erg/cm^2. Of course, entropy changes during wetting of clays may result not only from changes in water structure due to ion-water interactions, but also from interactions with surface charge sites and uncharged surface groups. Additionally, entropy changes may result from changes in the structure or arrangement of the solid phase or from redistributions of ions in the clay-water system (Kijne, 1969; Quirk, 1978).

Several studies have been reported in which entropy changes for water adsorption on clay minerals were investigated. van Olphen (1965) reported an entropy change of -7.4 cal deg^{-1}mole H_2O^{-1} for water adsorption on Na-vermiculite. Taking the area occupied by a water molecule as 6.25 $Å^2$ gives $-T\Delta S$ = +245 erg/cm^2. Increases in entropy have been reported for water adsorption on kaolinite (Martin, 1960). These entropy changes ranged from +28 cal deg^{-1}mole H_2O^{-1} at low surface coverages to about +2 cal deg^{-1}mole H_2O^{-1} at monolayer coverage. The average $-T\Delta S$ for adsorption of the first monolayer was about -200 erg/cm^2 and for subsequent adsorption between -15 and -70 erg/cm^2. Positive entropy changes of up to +15 cal deg^{-1}mole H_2O^{-1} have also been reported for water adsorption on Cs-, Rb-, and Li-

saturated montmorillonite at low surface coverages (Kijne, 1969). In the same study, Na-, NH_4-, and Ca-saturated montmorillonite, however, showed reductions in entropy at all surface coverages giving ΔS from -2 to -37 cal deg^{-1}mole H_2O^{-1}. After separating the entropy changes attributable to surfaces and cations, Kijne (1968) concludes that montmorillonite surfaces appear to have a structure making effect on water while kaolinite has a structure breaking effect.

The results of these and other such studies (Low and Anderson, 1958b; Barshad, 1960; van Olphen, 1969) suggest that at water contents near or below monolayer coverage, entropy changes are attributable largely to changes in water structure due to interactions with exchangeable ions and mineral surfaces--although changes in the solid phase should not be ruled out. These entropy changes may be positive or negative, but their absolute magnitudes are rather small (though not negligible) when compared with enthalpies of hydration in the same range of water contents.

At higher water contents, the redistribution of ions in the clay-water system may contribute significantly to the net entropy change. When in contact with pure water or dilute electrolyte, adsorbed ions will tend to diffuse away from the surface in response to solute concentration gradients. The distribution of ions in the so-called electrical double layer has been treated quantitatively by the Guoy-Chapman model (Verwey and Overbeek, 1948). The "effective thickness" of the diffuse ionic layer in the absence of interactions between adjacent surfaces is equivalent to the Debye-Hückel reciprocal length $1/\kappa$ given by:

$$1/\kappa = \left[\frac{\varepsilon kT}{e^2 \sum n_i v_i^2}\right]^{1/2} \qquad [9]$$

where ε is the permittivity of the medium, k is Boltzmann's constant, T is the absolute temperature, e is the electronic charge, and n_i and v_i are the number of ions per unit volume and valence, respectively, of ions in bulk solution.

It can be shown that the process of diffuse double layer formation is an entropic phenomena. At constant temperature and system composition the change in free energy is:

$$\begin{aligned} dG &= (\partial G/\partial p)\, dp \\ &= \bar{V}\, dp \end{aligned} \qquad [10]$$

We may consider the free energy change associated with diffuse double layer formation to be the reversible work done against an osmotic pressure. Substituting the osmotic pressure Π for p, and assuming the molar volume $\bar{V}$ to remain constant gives:

$$\Delta G = \Pi \bar{V} \qquad [11]$$

Furthermore, at low solute concentrations, we find that:

$$\Pi \bar{V} = RT \qquad [12]$$

which is known as the van't Hoff equation. At constant external pressure:

$$S = -(\partial G/\partial T)_p \qquad [13].$$

Combining Equations 11 and 12 and integrating gives $S = -R$. Combining this finding with Equations 11 and 12 and the basic thermodynamic expression:

$$G = H - TS \qquad [14]$$

we see that for osmotic phenomena:

$$\Delta G = -T\Delta S \qquad [15]$$

This fact bears importance to the effect of temperature on water adsorption and associated swelling. It may also explain the much higher water adsorption from the liquid phase than from vapor observed by Emerson (1962a,b) for Ca-montmorillonite. Perhaps diffuse double layers do not develop fully in equilibrium with vapor because of the considerably greater entropy of water in the gaseous state than in the liquid state.

Mechanisms of Swelling

If swelling accompanies wetting, clearly water adsorption must either directly or indirectly increase the repulsive forces between mineral particles, decrease the attractive forces, or both. We have considered in detail the forces responsible for water adsorption. These forces may be viewed as contributing to interparticle repulsion to the extent that adsorption occurs by intercalation of water between adjacent surfaces. Before delving into an analysis of the mechanisms of soil volume changes, we need to first briefly examine the nature of the interparticle attractive forces which counteract expansive forces.

Interparticle attractive forces

Attractive forces between adjacent mineral particles arise through the same general mechanisms of interaction which were discussed in the preceding sections. The most significant of these are van der Waals and Coulombic forces and forces arising from surface tension at air-water interfaces.

The magnitude of van der Waals attraction between bodies larger than atomic dimensions will be considerably greater than for two single atoms because many interacting atomic pairs contribute to the total attraction. The van der Waals interaction energy per unit area (E/a) between two semi-infinite plates of finite thickness, for example, is given by:

$$\text{E/a plate-plate} = \frac{A}{12\pi}\left[\frac{1}{x^2} + \frac{1}{(x+2\delta)^2} - \frac{2}{(x+\delta)^2}\right] \qquad [16]$$

where x is the plate separation, δ is the plate thickness and A is the Hamaker constant, which is an aggregate of coefficients reflecting the combined effects of London, Debye and Keesom interactions (Verwey and Overbeek, 1948; Hiemenz, 1977). This relation holds for distances up to about 100-200 Å after which retarded van der Waals forces come into play (Tabor and Winterton, 1968). Direct measurements of forces between mica surfaces separated by water have yielded a Hamaker constant of 2.2 x 10^{-20} J (Israelachvili and Adams, 1978).

When interparticle spacings are less than about 10 Å, it seems likely that exchangeable ions will occupy a plane midway between the two surfaces. These ions would be mutually attracted to both surfaces by electrostatic forces (Norrish, 1954; van Olphen, 1965) as given by Equation 6. For a cation interacting with two negative surfaces each proferring a charge equal to half the ion's valence (v), the equation describing the interaction energy per unit area (E/a) between the surfaces due to "cation-bridging" is:

$$E/a_{\text{cation bridge}} = - \frac{ve\sigma}{8\pi\epsilon x} \qquad [17]$$

in which σ is the surface charge density. It is seen that cation-bridging energy increases with cation valence and surface charge and decreases with separation distance. Point-charge separation distance will depend on the cation size (hydrated or unhydrated radius as the case may be) and on the origin of charge. Accordingly, a tetrahedrally substituted montmorillonite should exhibit stronger cation-bridging than an octahedrally substituted sample of similar surface charge (Eisenman, 1962). When ions cease to occupy the midplane between adjacent surfaces, Equation 17 will

no longer be valid and the contribution of cation-bridging to attractive energy will diminish rapidly.

In the same manner that two negative planar surfaces may interact via intermediate cations, positive surfaces may bind together through adsorbed anions. This may, for example, result in edge-to-edge bonds between phyllosilicate clays at low pH. Coulombic attraction may also result in edge-to-face bonds between phyllosilicate clays when positive edges interact directly with negative planar faces (Norrish and Rausell-Colom, 1963; Rowell, 1965; Roberson et al., 1968).

In unsaturated soil-water systems, a cohesive force will occur between the solids due to unbalanced molecular forces at liquid-gas phase boundaries (Baver et al., 1972; Kirkham and Powers, 1972). Consider as an example the force which develops between two parallel discs as shown in Figure 2. A pressure deficit (p) exists in the water film which is given by the Laplace equation:

$$p = \gamma \left[\frac{1}{r} - \frac{1}{a} \right] \qquad [18]$$

where γ is the surface tension, r is the meniscus radius and a is the disc radius. If the contact angle is zero, then the interplate distance (x) equals 2r and

$$p = \gamma \left[\frac{2}{x} - \frac{1}{a} \right] \qquad [19]$$

A force (f) acts along the air-water interface and is equal to the product of meniscus circumference and surface tension

$$f = \gamma \, 2\pi(a-x) \qquad [20]$$

Dividing this force by the plate area and adding it to the Laplace pressure gives the total capillary cohesion per unit area (P):

$$P = 2\gamma \left[\frac{1}{x} + \frac{a-x}{a^2} - \frac{1}{2a} \right] \qquad [21]$$

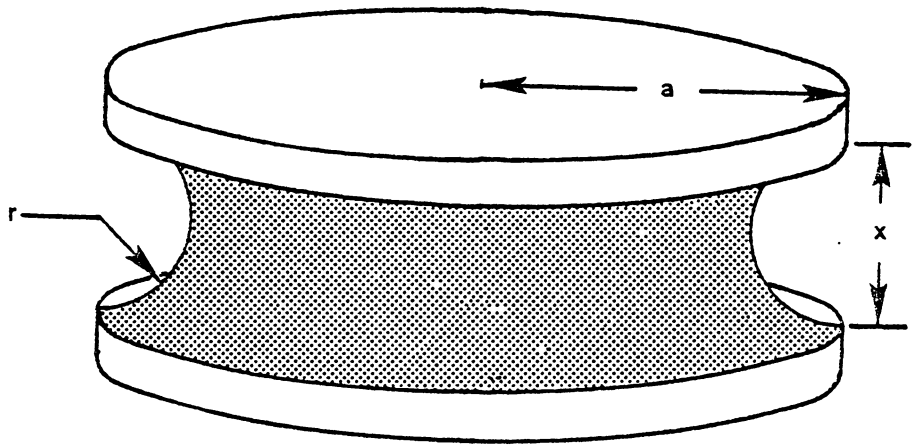

Figure 2. Capillary cohesion between two parallel discs.

For values of $x \ll a$, the first term in the brackets is dominant and the cohesive force decreases linearly with increasing plate separation, while the interaction energy accordingly decreases logarithmically.

Crystalline swelling

Norrish (1972) has termed swelling that accompanies adsorption of the first two to three water layers by intercalation between unit layers of phyllosilicate clays as "crystalline swelling." Under normal conditions, only montmorillonites and vermiculites exhibit such behavior. Their equilibrium c-axis spacings, which vary with mineral and exchangeable ion species, relative vapor pressure and temperature (Eisenman, 1962; Kittrick, 1969a; Keren and Shainberg, 1975), have been viewed as the net result of expansive forces arising from mineral surface and exchangeable ion hydration energies, and contractive forces attributed to Coulombic and van der Waals attractions between surfaces (Sposito and Babcock, 1966; Kittrick, 1969b).

From a knowledge of the mechanisms involved in crystalline swelling, the effects various factors have on it can be estimated. Increasing surface charge, for example, should increase the expansive forces arising from cation and charge site hydration. However, the contracting force due to cation bridging also increases with the net result generally being in favor of reduced expansion with increasing surface charge--at least in the range of surface charges occurring on montmorillonites and vermiculites. Increasing tetrahedral layer charge at the expense of octahedral charge would be expected to increase exchange site hydration energy and cation bridging--again the latter generally predominating, resulting in diminished expansion. An increase in exchangeable ion valence will

increase ion hydration energy as well as cation bridging. Comparison of Equations 4 and 5, which describe ion hydration, with Equation 6, which describes ion-surface interaction, suggests that contractive forces may increase to a greater extent than expansive forces as counterion valence is increased. Increasing counterion size will reduce ion hydration energy, while the effect on cation-bridging energy will depend upon crystal separation distance.

Osmotic swelling

Swelling of clay minerals beyond the so-called crystalline region has been considered to be osmotic in nature by a number of workers (Schofield, 1946; Bolt and Peech, 1953; Ruiz, 1962; El-Swaify and Henderson, 1967; Norrish, 1972; van Olphen, 1975). A quantitative analysis of the interaction between adjacent double layers was developed by Derjaguin and Landau (1941) and Verwey and Overbeek (1946; 1948) and is frequently referred to as the DLVO theory. The repulsive force between two charged parallel plates is considered to arise from an osmotic pressure caused by a difference between the electrolyte concentration in bulk solution and at a plane midway between the two plates. Combining the van't Hoff equation for osmotic pressure with an expression for midplane ion concentration from double layer theory gives the repulsive force per unit area (P_r):

$$P_r = 2nkT\ (\cosh u - 1) \qquad [22]$$

where n is the number of ions per unit volume in bulk solution, kT is the thermal energy, and $u = ve\psi_m/kT$ in which ψ_m is the midplane electrical potential. The value of ψ_m varies with the separation distance (x) between the plates according to:

$$x = -\frac{2}{\kappa}\left[\frac{dv}{[2(\cosh y - \cosh u)]^{1/2}}\right] \qquad [23]$$

in which κ is the Debye-Hückel parameter (Equation 9), $y = ve\psi/kT$ where ψ is the potential at any given distance from the surface, and $z = ve\psi_o/kT$ where ψ_o is the potential at the surface (or more properly the Stern boundary). The value of ψ_o for constant charge minerals is obtained from the Gouy-Chapman equation:

$$\sigma = (2n\varepsilon kT)^{1/2} \sinh (ve\psi_o/2kT) \qquad [24]$$

where σ is the diffuse layer charge density. Tabulated solutions to Equation 23 have been given by Verwey and Overbeek (1948), van Olphen (1963), Kemper and Quirk (1970), and Bresler (1972).

In the DLVO theory, the attractive force per unit area (P_a) between parallel plates is considered to arise from van der Waals interactions and is given by the derivative of Equation 16:

$$P_a = -\frac{A}{6\pi}\left[\frac{1}{x^3} + \frac{1}{(x + 2\delta)^3} - \frac{2}{(x + \delta)^3}\right] \qquad [25]$$

Summing the attractive and repulsive forces given by Equations 22 and 25 yields a theoretical function for net interparticle force versus plate separation distance. Experimental verification of the DLVO model has been attempted by a number of researchers in the last 25 years (Bolt and Miller, 1955; Warkentin et al., 1957; Norrish and Rausell-Colom, 1963; Barclay et al., 1970; Barclay et al., 1972; Walker, 1975). The results show fair agreement between theory and experiment for Na-montmorillonite and Li-vermiculite, if all exchangeable ions are assumed to occur in the diffuse double layer. Measured swelling pressures for

Ca-montmorillonite, however, have been found to be far below predicted DLVO values (Warkentin et al., 1957).

X-ray diffraction studies suggest that Ca-montmorillonite exhibits an energy minimum deep enough to restrict expansion beyond an interlayer spacing of $\sim$ 10Å following initial platelet collapse (Keren and Shainberg, 1975). Differences between interaction energy functions of Na- and Ca-saturated montmorillonite in contact with dilute electrolyte are illustrated qualitatively in Figure 3. The energy minimum for Ca-montmorillonite results from the contribution of cation bridging at small separation distances which is not considered in the DLVO model. Once the energy barrier between the metastable dispersed state and the face-to-face flocculated state is overcome, diffuse double layer development on collapsed faces will no longer occur. The resultant groups of oriented platelets which exhibit limited interlayer expansion have been variously referred to as domains, turbostratic groups, tactoids, and quasicrystals (Quirk and Aylmore, 1960; Aylmore and Quirk, 1960; Blackmore and Miller, 1961; O'Conner and Kemper, 1969). By hypothesizing the existance of "tactoids" composed of neatly stacked platelets which develop diffuse double layers on external surfaces only, Blackmore and Miller (1961) were able to achieve more reasonable agreement between measured swelling pressures of Ca-montmorillonite and pressures calculated from DLVO theory.

In systems which exhibit limited interlayer expansion following initial platelet contraction, two components of water adsorption and swelling may be theoretically distinguished. One is due to adsorption on internal surfaces and is restricted to a few water layers. The

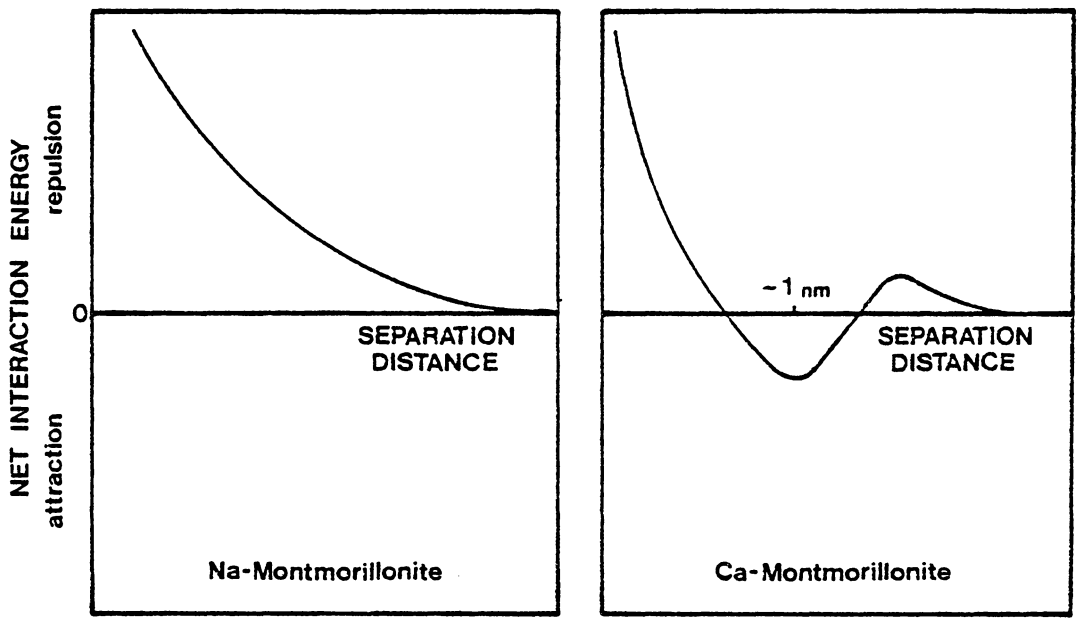

Figure 3. Interaction energies versus plate separation distance for Na- and Ca- saturated montmorillonite in contact with free water at room temperature.

second is due to adsorption on external surfaces which are unconstrained by planar surface interactions. The first has been referred to as intracrystalline adsorption and the latter as intercrystalline adsorption by Rowell (1965). Considerable disagreement occurs in the literature regarding the relative contributions of intracrystalline and intercrystalline adsorption to total adsorption and volume change. Aylmore and Quirk (1962) postulated that diffuse double layer formation is of little significance in systems with divalent exchangeable cations, whereas van Olphen (1975) has suggested that osmotic adsorption is the predominant cause of soil swelling. In a statistical study, Greene-Kelly (1974) concluded that intracrystalline shrinkage accounted for only a fraction of the total shrinkage from pF 4 to 6. Schafer and Singer (1976), however, reported fair success with a predictive model which assumed all soil volume change resulted from intracrystalline swelling.

Other swelling mechanisms

Although deficiencies in double layer theory have long been recognized (Bolt and Peech, 1953; Bolt, 1955; Low, 1959; Rosenquist, 1962), a large portion of the scientific community has held to the opinion that swelling beyond the crystalline region is chiefly an osmotic phenomenon. This concept has been questioned, however, and a number of alternative mechanisms suggested.

Clay-water epitaxy. Low and his coworkers at Purdue University have recently contended that osmotic phenomena cannot contribute significantly to clay swelling (Low and Margheim, 1979; Low, 1980). They base this on the hypothesis that most exchangeable ions reside in the

Stern layer rather than the diffuse layer and therefore cannot contribute to osmotic pressures. If their estimations are correct, midplane potentials and thus osmotic pressures calculated by Equation 22 would fall far below measured swelling pressures even for such model systems as Na-montmorillonite.

Low suggests that the predominant mechanism of water adsorption and associated swelling involves water-surface interactions which result in epitaxy between the surface and water structure extending at least 50 Å from the surface (Ravina and Low, 1977; Low and Margheim, 1979). Two general lines of evidence have led to this hypothesis: (1) apparent differences between properties of bulk and adsorbed water (viscosity, density, specific heat, heat of compression, entropy, etc.) up to high water contents (Low and Anderson, 1958a; Kolaian and Low, 1960; Kay and Low, 1975; Low, 1979) and (2) apparent relationships between crystal b-dimensions and swelling. The latter includes an apparent inverse relationship between dry b-dimension and free swelling, and between wet b-dimension and water content. Both lines of evidence remain controversial. Hawkins and Egelstaff (1980) concluded from neutron diffraction studies that a and b dimensions of the montmorillonite they studied did not vary with moisture content and that water-surface interactions caused no structural perturbations beyond the first water layer. Reviews of water adsorption on clays by Martin (1962), Graham (1964), and van Olphen (1975) stress that evidence regarding the nature of adsorbed water is either ambiguous or inconclusive. These uncertainties remain to be elucidated.

Strain relaxation and differential strain. Water-surface interactions are not the only alternative mechanism to osmotic adsorption and swelling. Terzaghi (1927) reasoned that particle distortions would accompany increases in applied stress, and that upon unloading, more or less elastic rebound of the distorted crystals would result in expansion of the mass. Aylmore and Quirk (1960) have suggested that drying may similarly induce crystal distortions which undergo relaxation upon wetting, resulting in the release of mechanical energy.

Another possible mechanism of swelling accompanying wetting involves differential strain between adjacent particles or groups of particles within a clay mass. The following scenario has been suggested by Rowell (1965). Consider two crystals at time t_o prior to wetting as shown in Figure 4. At time t_1, the crystal on the left is wetted and swells. As wetting proceeds, the crystal on the right expands at time t_2. However, edge-to-edge bonds cause the crystal on the left to be pulled further apart when the crystal on the right expands. Differential strains between crystals or groups of crystals can readily be visualized for more random particle orientations than envisioned by Rowell. Quirk (1978), for example, has suggested that randomly packed "domains" of oriented crystals will undergo rotational and translational displacements during wetting resulting, as in Rowell's mechanism, in an increase in the volume of relatively large pores and the quantity of water held by capillarity.

Capillary forces. Quirk (1978) observed that swelling of a Ca-illite occurred largely by expansion of pores in the range 100-1000 nm and suggested that capillary phenomena were implicated. Capillary

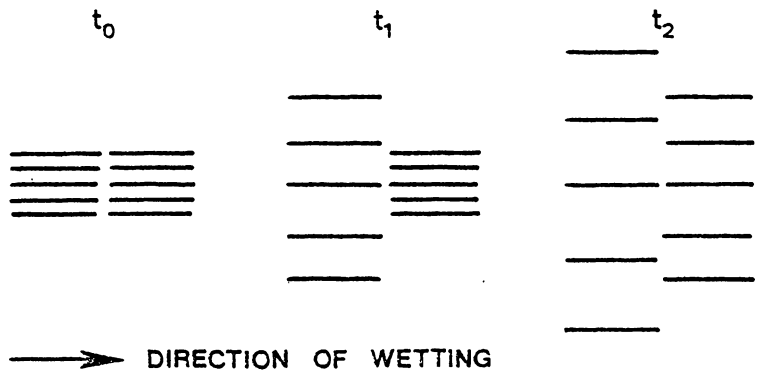

Figure 4. Swelling due to edge-to-edge bonds during wetting (after Rowell, 1965).

phenomena may induce expansion during wetting in one of two ways: (1) by reducing capillary cohesion, hence increasing net repulsion, or (2) by inducing swelling pressures in entrapped air. This first process results from a reduction in the area of air-water interfaces at high water contents causing a reduction in capillary cohesion. The second process involves the buildup of pressure in air trapped ahead of an advancing wetting front (Stroosnyder and Koorevaar, 1972). The situation may be modeled by consideration of a cylindrical capillary of radius r which is wet from both ends simultaneously. The force vector F_γ along the axis of the capillary due to surface tension at the air-water interface is:

$$F_\gamma = 2\pi r \gamma \cos \theta \qquad [26]$$

where γ is the surface tension and θ is the contact angle. The opposing force F_p arising from the pressure p in the trapped air, in excess of the hydrostatic pressure, is:

$$F_p = p\pi r^2 \qquad [27].$$

When the meniscus is stationary, $F_\gamma = F_p$; hence:

$$p = \frac{2 \gamma \cos \theta}{r} \qquad [28]$$

which is recognized as a form of the Laplace equation. Thus, during wetting, a pneumatic pressure given in the ideal case by Equation 28 may develop which contributes to soil swelling. A reduction in swelling of montmorillonite caused by evacuation prior to submersion observed by Emerson (1964) supports the hypothesis that entrapped air pressures may result in expansion.

Swelling and Microstructure

It should be evident from the foregoing discussions that the microstructure of a system will greatly affect water adsorption and swelling. In systems which exhibit limited interlayer expansion following initial platelet contraction, the magnitude of intracrystalline and intercrystalline water adsorption and associated swelling will vary with the ratio of external to internal surface area, which depends on the degree of platelet orientation. As Aylmore (1977) has pointed out, however, it is unrealistic to visualize clay structure as consisting of neatly stacked booklets of oriented platelets grouped together in random array as hypothesized by Blackmore and Miller (1961). Common sense dictates that some bending, twisting, and interleaving of platelets is probable and that the boundaries between adjacent "tactoids" or "quasicrystals" and between external and internal surface areas may not be readily discernable or entirely tangible.

Supported by neutron diffraction experiments and electron microscopic evidence, Cebula et al. (1979) presented a model of clay structure which consists of overlapping regions of oriented platelets interspersed with voids, regions of gross folding, edge-to-face stacking and disordered stacking. Norrish and Rausell-Colom (1963) and Rowell (1965) among others have indicated that edge-to-face bonds may inhibit expansion by binding crystals into a more rigid network. Edge-to-edge bonds, on the other hand, have been associated with a mechanism by which increased expansion may occur (Rowell, 1965).

The size of voids within a soil or clay sample may greatly affect the magnitude of swelling and its relation to water adsorption. Clearly, for water adsorption to directly induce expansion, adsorption must occur by intercalation between adjacent surfaces--that is, by mutual repulsion of contiguous water layers. Water retained in larger pores by capillarity cannot contribute to such interaction since it exists in a state of tension. Thus, conceptually at least, a distinction may be drawn between water adsorbed by capillarity and that associated with mineral surfaces--whether through double layer development, surface-water epitaxy, or some other mechanism. The occurrence of significant quantities of such "non-associated" or "occluded" water has been inferred by Bolt and Miller (1955), Blackmore and Miller (1961) and Rowell (1963) to occur in montmorillonite pastes even after increasing particle orientation by precompression or other means.

In reality, the delineation between capillary and surface-associated water is one that is difficult, if not impossible, to circumscribe. Furthermore, as the previous discussion of capillary swelling has indicated, water adsorption by capillarity may itself significantly effect expansion. As Equation 28 indicates, swelling due to entrapped air pressures may increase as pore size diminishes. It is conceivable that decreasing capillary cohesion during wetting could permit relaxation of strained crystals and perhaps reorientation of groups of crystals which would result in bulk expansion.

Micromorphology will be greatly affected by stress history, as well as by the surface chemistry, morphology and size distribution of the solids. Roberson et al. (1968) and Cebula et al. (1979) have

reported that the frequency of face-to-face, edge-to-edge, and edge-to-face orientations differ for various size fractions of montmorillonite. Blackmore and Miller (1961) found that precompression increased the number of platelets per "tactoid" for Ca-montmorillonite estimated from x-ray diffractogram peak widths and suggested that osmotic water adsorption would thereby be reduced. Compaction, however, has been observed to cause increases as well as decreases in the volume changes of various soils (Schmertmann, 1973; Parker et al., 1977).

Changes in structure which accompany drying of soils and clays may affect the magnitude of expansion on rewetting. Parallel orientation may be induced by drying of dispersed clays (Rowell, 1963). However, Cebula et al. (1979) have reported that suction was less effective than compression in causing increased orientation. Although changes in microstructure which accompany shrinking and swelling are not likely to be entirely reversible, after repeated cycles of wetting and drying, shrinkage and swelling become very nearly equal (Ring, 1965).

METHODS AND MATERIALS

Experiment 1: Water Adsorption and Swelling of Ca-montmorillonite Compacted to Different Densities

Theoretical

Osmotic and intracrystalline components of water adsorption by Ca-saturated montmorillonite (Ca-MT) was calculated by assuming the existance of discrete crystals which develop fully extended, diffuse double layers on external surfaces but undergo limited intracrystalline expansion. From geometrical considerations, intracrystalline adsorption by such a system will be given by the produce of internal surface area and one-half the interlayer separation. Osmotic adsorption will equal the product of external surface area and double layer thickness.

Crystal expansion associated with intracrystalline water adsorption was calculated as the product of internal surface area and one-half the change in interlayer separation, while an estimate of expansion attributable to double layer extension was taken equal to the predicted volume of osmotic water adsorption. Conversions from volume to mass of adsorbed water, and visa versa, were made by assuming a water density of 1.0 g/cm^3.

Low temperature N_2 adsorption BET surface area was taken as a measure of external surface area (Emerson, 1962a; van Olphen, 1975). Internal surface area was calculated as the difference between total surface area taken to be 800 m^2/g and N_2 surface area. Interlayer spacing was computed as the difference between c-acis spacing from x-ray diffraction analysis (XRD) and the solid crystal thickness taken

as 9.6 Å. Double layer thickness was calculated as the sum of Stern layer thickness taken to be 5 Å (approximately two water layers) and Gouy layer thickness ($1/\kappa$) calculated as:

$$1/\kappa = (\varepsilon kT/e^2 \sum_i n_i v_i^2)^{1/2} \quad [29]$$

where ε is the permittivity of the medium, k is Boltzmann's constant, T is the absolute temperature, e is the electronic charge, and n_i and v_i are the number of ions per unit volume and the valence of ions, respectively, in bulk solution. Permittivity is the product of relative permittivity taken as 80 and the permittivity of free space.

Experimental

Wyoming montmorillonite (Clay Minerals Society Source Clay Repository SWy-1) was Ca-saturated by washing three times with 1 N $CaCl_2$ followed each time by centrifugation and decantation. Excess salts were removed with distilled water washes followed by 1:1 water-methanol and acetone washes until a negative $AgNO_3$ test was obtained. The 80°C-dried clay was gently ground with a mortar and pestle and stored in a desiccator over P_2O_5.

Cores measuring 36 mm in diameter and 10 mm in height were prepared by static compaction of P_2O_5-dry Ca-MT in 38 mm tall stainless steel rings by means of a hydraulic press. The bottom of each ring was secured to a 6 mm thick porous stone. Quantities of clay added to each ring were adjusted to yield cores with densities ranging from approximately 0.50 to 1.60 g/cm^3. Densities were expressed on a 105°C-dry basis by correcting for the moisture content of P_2O_5-dry clay

which was found to be 0.08 g/g. A 0.5-1.0g subsample from each core was carefully chipped loose so as to minimize disturbance of the clay structure and saved for N_2 adsorption measurements. The holes in the cores were refilled with the same quantity of clay that was removed. Porous stones of 35 mm diameters were placed inside each ring on top of the core, and initial height readings were made to the nearest 0.001 inch with a tripod-mounted strain guage.

Cores having initial densities of 0.52, 0.75, 1.06, 1.37 and 1.59 g/cm^3 were submerged in 0.01 N $CaCl_2$. A second core of density 1.06 g/cm^3 was submerged in 0.001 N $CaCl_2$ and a third in 0.01 N $Ca(H_2PO_4)_2$. A fourth core was allowed to adsorb water vapor for 5 weeks in a desiccator containing distilled water, after which 0.01 N $CaCl_2$ was added to the sample a few drops a day for several weeks until free solution was ponded on the top porous stone.

At the completion of each test, height readings of the samples were taken from which final volumes were calculated. Specific volume change was calculated as the change in volume per unit mass of 105°C-dry clay. Portions of each core were freeze-dried following immersion in liquid N_2 and saved for surface area and pore size distribution analyses. Total water adsorption was taken equal to the final void volume, computed as the difference between total final volume and the calculated volume of the solids. Specific gravity of 105°C-dry clay was found to be 2.70 g/cm^3 by water displacement in 25 ml pycnometers.

Interlayer separations of wet and dry Ca-MT were measured by XRD of oriented clay mounted on ceramic tiles by vacuum filtration of suspensions. The c-axis spacing of wet clay was measured on a sample which was sprayed with a water mist just prior to being scanned in an enclosed goniometer chamber containing a vessel of distilled water. After drying, the c-axis spacing was determined again in a closed goniometer chamber containing P_2O_5.

Nitrogen gas adsorption measurements were performed with a Micromeritics Model 2100-D gas adsorption apparatus. Samples were degassed overnight at 200°C to a pressure of <2μm Hg. Isotherms were determined at liquid N_2 temperatures which were measured to the nearest 0.01°C. Surface areas were calculated by analyzing adsorption data in the range 0.05 to 0.30 p/p_o by application of the BET equation:

$$\frac{p/p_o}{V_a(1 - p/p_o)} = \frac{1}{cV_m} + \frac{(c - 1)p/p_o}{cV_m} \qquad [30]$$

where p/p_o is the relative vapor pressure, V_a is the volume of gas adsorbed, V_m is the volume of gas adsorbed at monolayer coverage, and c is a constant. Surface areas were calculated from V_m on the assumption that each molecule of N_2 occupied 16.2 $Å^2$ of surface.

Complete N_2 gas adsorption and desorption isotherms were measured for the samples taken from cores prior to wetting. The distributions of pores in the range 10-1000 Å were calculated from desorption data by employing the Kelvin equation, assuming a pore geometry consisting of parallel slits, and correcting for film thickness not attributable to capillary condensation (Aylmore, 1974):

$$d - 2t = \frac{-2\ \bar{V}\ \gamma\ \cos\ \theta}{RT\ \ln\ p/p_o} \qquad [31]$$

in which d is the plate separation, t is the non-capillary film thickness, $\bar{V}$ is the molar volume of liquid N_2, γ is the surface tension, θ is the contact angle (assumed zero), R is the gas law constant, and T the absolute temperature. The value of t in Å was calculated from the Halsey-type expression:

$$t = 3.54\ (-2.58/\ln\ p/p_o)^{0.45} \qquad [32]$$

derived from data compiled by Adamson (1976) for N_2 adsorption by various nonporous solids. Pore volumes were obtained by numerical integration of the expression:

$$v_1 - v_2 = \int_{d_2}^{d_1} \Delta S_p\ dd \qquad [33]$$

where v_1 and v_2 are the volume of pores smaller than d_1 and d_2, respectively, and ΔS_p is the surface area of pores of a specific size calculated as:

$$\Delta S_p = \frac{\Delta V - \Delta t \Sigma \Delta S_p}{(d - 2t)_{avg}} \qquad [34]$$

where ΔV is the incremental volume of desorbed N_2, Δt is the corresponding change in film thickness, $\Sigma\Delta S_p$ is the surface area of emptied pores, and $(d - 2t)_{avg}$ is the average Kelvin pore size for the desorption decrement.

Pore size distributions were also determined for several samples by Hg intrusion porosimetry by application of the Young-Laplace equation:

$$d = P/2\ \gamma_{Hg} \cos \theta \qquad [35]$$

where d is the plate separation, P is the pressure, γ_{Hg} is the surface tension of Hg and θ is the contact angle between Hg and clay which was assumed to be 140°.

Experiment 2: Water Adsorption and Swelling of Montmorillonite and Vermiculite with Different Exchangeable Ions

Theoretical

Osmotic and intracrystalline components of water adsorption and swelling by Ca- and Al-saturated montmorillonite (Ca-MT and Al-MT) and Na-, Ca-, and Al-saturated vermiculite (Na-VR, Ca-VR, and Al-VR) were calculated by the same procedure outlined in Experiment 1 for crystals exhibiting limited intracrystalline expansion. Total surface areas of both montmorillonite and vermiculite were assumed to be 800 m^2/g.

For Na-saturated montmorillonite (Na-MT), diffuse double layer formation was considered to occur on all platelet surfaces in the presence of dilute electrolyte. Osmotic adsorption and expansion of Na-MT were thus calculated as the product of total surface area and double layer thickness. Intracrystalline adsorption and expansion were considered non-existant for Na-MT.

Experimental

The clay minerals used in this study were a Wyoming montmorillonite (Clay Minerals Society Source Clay Repository SWy-1) and a South Carolina vermiculite (Zonolite). The vermiculite was first comminuted by stirring a slurry in a high speed mixer. The clay fraction was separated by centrifugation of suspensions dispersed in water adjusted to pH 10 with Na_2CO_3. X-ray diffraction and total elemental analysis indicated that the vermiculite was in fact a regularly interstratified vermiculite-mica. To eliminate the interstratification, the material was boiled in 0.1 N $BaCl_2$ until the double XRD peak at 14.2 and 12.0 Å

of Mg-saturated, glycerol-solvated clay was replaced by a single 15.0 Å peak. The process took several weeks during which time the $BaCl_2$ solution was decanted and replaced by fresh solution daily.

Aliquots of the montmorillonite and vermiculite were saturated with Na, Ca, or Al by washing three times with 0.5 N solutions of the chloride salts. Excess salts were removed with water washes followed by ethanol washes until a negative $AgNO_3$ test was obtained. After the last wash, the samples were redispersed in water, frozen and dried by sublimation under vacuum. The samples were stored in containers exposed to ambient room temperature and humidity.

Moisture contents of the Na-, Ca-, and Al-saturated montmorillonite and vermiculite were obtained by drying subsamples in a 105°C oven prior to preparation of compacted cores. Quantities of each clay were added to 36 mm diameter by 38 mm high stainless steel rings to give sample weights of 10 g on a 105°C-dry basis. The bottom of each ring was secured to a 6 mm thick porous stone. After compressing samples with a hydraulic press to yield bulk densities of 0.98 ± 0.02 g/cm^3, a 0.5-1.0 g subsample from each core was chipped loose. The subsample was saved for N_2 gas adsorption measurements and scanning electron microscopy, and the holes in the cores were refilled with the same quantity of clay that was removed. A 35 mm diameter porous stone was placed inside each ring on top of the core, and initial sample heights were determined to the nearest 0.001 inch with a tripod mounted strain gauge.

Cores of the Na-, Ca-, and Al-saturated montmorillonite and vermiculite were placed above distilled water in a desiccator subject

to room temperature. Weight and height readings were recorded for 7 months until they no longer increased. Following vapor adsorption, solutions of 0.01 N chloride salts of the same cation present on the exchange complex were added incrementally to each core. Every day for 3 months, 4 drops of the appropriate solution were added to the top of each core, after which the cores were submerged in 0.01 N salt solutions. The containers were covered to reduce evaporation and the solutions drained and replaced weekly for 10 weeks, after which sample heights were again determined. A portion of each core was used to determine the final moisture content by drying to 105°C.

A second core of Ca-MT was subjected to a vacuum-wetting treatment. A core prepared in the same manner as the others was evacuated overnight in a desiccator at a pressure of <10 μm Hg. A solution of 0.01 N $CaCl_2$ was then introduced into the desiccator through a two-way stopcock. The submerged core was allowed to equilibrate 7 days after which the sample height was measured with a dial gauge. The height was checked again at 10 and 14 days and found stable. The sample was removed from the ring and the final moisture content determined gravimetrically.

The c-axis spacings of wet Na-, Ca-, and Al-saturated clays were measured by XRD as in Experiment 1. Air-dry and 105°C-dry spacings were also determined. Room temperature and relative humidity at the time air-dry spacings were measured were 22°C and 27%, respectively. N_2 adsorption surface areas were determined in the same manner as in Experiment 1. Micrographs of Au-Pd-coated samples of the compacted clays prior to wetting were taken with a model AMR 900 scanning electron microscope.

Experiment 3. Water Adsorption and Swelling of Compacted and Undisturbed Iredell and Poplimento B2 Horizons

Theoretical

Osmotic and intracrystalline components of water adsorption and swelling of two soils containing various amounts of montmorillonite (MT) and vermiculite (VR) were calculated in a manner similar to that in the first two experiments dealing with monomineralic systems. Osmotic adsorption was assumed to occur on external surfaces of MT and VR and intracrystalline adsorption on internal surfaces. The average external surface area of MT and VR crystals per unit mass of soil (S_E) was calculated as:

$$S_E = S_{N2} - S_o \qquad [36]$$

where S_{N2} is the specific surface area of the whole soil measured by N_2 adsorption and S_o is the surface area of soil components other than MT and VR. The value of S_o was computed as:

$$S_o = \frac{m_s}{m_t} S_s + \frac{m'_{si}}{m_t} S'_{si} + \frac{m'_c}{m_t} S'_c \qquad [37]$$

where m_s/m_t and S_s are the mass fraction and specific surface area, respectively, of the sand fraction, m'_{si}/m_t and S'_{si} are the mass fraction and specific surface area of silt size minerals excluding any MT and VR, and m'_c/m_t and S'_c are the mass fraction and specific surface area of clay size minerals other than MT and VR. S_s was taken to be zero; S'_{si}, which is determined in these soils largely by quartz and to a lesser extent mica, was taken as 1 m^2/g; and S'_c, attributable largely to kaolinite, mica and some quartz, was taken as 10 m^2/g.

Average internal surface areas of MT and VR crystals per unit mass of soil (S_I) were calculated from:

$$S_I = S_T - S_{N2} \qquad [38]$$

where S_T is the total specific surface area of the whole soil given by:

$$S_T = \frac{m_{MT}}{m_t} S_{T/MT} + \frac{m_{VR}}{m_t} S_{T/VR} + S_O \qquad [39]$$

in which m_{MT}/m_t and m_{VR}/m_t are the mass fractions of MT and VR, and $S_{T/MT}$ and $S_{T/VR}$ are the total specific surface areas of MT and VR taken equal to 800 m^2/g.

Osmotic adsorption and swelling were calculated as the product of double layer thickness and S_E. Diffuse double layer thicknesses were calculated for the multi-ionic equilibrating solutions by noting that ionic strength (I) is given by:

$$I = \sum_i n_i v_i^2 / 2N_a \qquad [40]$$

where n_i and v_i are the number of ions per unit volume and the valence of ions in solution and N_a is Avogadro's number. Combining this with Equation 29 gives:

$$1/\kappa = (\varepsilon kT/2e^2 N_a I)^{1/2} \qquad [41]$$

Intracrystalline adsorption was calculated as one-half the product of internal surface area and the mean crystal separation distance of expansive 2:1 phyllosilicates. Intracrystalline swelling was taken as one-half the product of internal surface area and the change in mean crystal separation distance of expansive 2:1 minerals.

Experimental

Undisturbed 3-inch thin-wall tube and bulk samples from B2t horizons of an Iredell (fine, montmorillonitic, thermic Aquic Hapludalf) and Poplimento (fine, mixed, mesic Ultic Hapludalf) pedon were taken in Loudoun and Pulaski Counties, Virginia, respectively. The thin-wall tubes were sealed with parafin in the field to prevent drying. The bulk samples were air-dried and ground through a 2 mm screen. Particle size distribution was determined by the pipette method. Moisture-density relations were determined by the miniature Harvard procedure using a compactive effort of 88 N per tamp with 25 tamps per each of 5 layers.

Free Fe contents in the soils were determined by atomic absorption analysis of dithionite-citrate-bicarbonate (DCB) extracts. Mineralogy of the silt and clay fractions was evaluated by XRD and differential scanning calorimetry (DSC). Silt and clay fractions were separated by wet sieving and centrifuging of DCB-treated soil. Oriented samples of K-saturated and Mg-saturated, glycerol-solvated (Mg-Gl) silt and clay were prepared by vacuum filtration on ceramic tiles. XRD patterns were obtained for air-dried and 105°C-dried Mg-Gl samples and for air-dried, 105, 300, and 550°C-dry, K-saturated samples using Cu Kα radiation. Kaolinite was determined quantitatively by DSC and used as an internal standard to semiquantitatively estimate proportions of other minerals from XRD peak areas.

Cores of the two soils were prepared by compaction in miniature Harvard molds at optimum moisture and above and below optimum at moisture contents corresponding to 90% of maximum density. After

extruding the cores from the molds, each was broken into two clods. Clods of undisturbed soil, about 30-50 cm^3 in volume, were removed from the thin-wall tubes. Clods prepared by compaction at optimum moisture will be referred to as CO samples and those compacted to 90% of maximum density, below and above optimum, will be termed CL and CH clods, respectively. Subsamples of the CL, CO, and CH clods and the undisturbed clods were 105°C oven-dried to determine moisture content. Other subsamples were freeze-dried and saved for N_2 gas adsorption measurements.

After determining the initial weights of the clods, they were placed in hair nets and coated with Saran by dipping them in a 1:5 mixture of Saran resin and 2-butanone. Initial clod volumes were then determined by weighing them suspended in water, using Archimedes' principle. Holes were pricked in the Saran coatings, and the clods were submerged in 0.01 M ionic strength solutions approximating the natural soil solutions (see Appendix). The solutions were drained and removed after 5 and 10 days, and after 15 days the final volumes were determined in the same manner as before.

The clods were then allowed to air-dry for 15 days before recoating with Saran and redetermining volumes. Holes were again pricked in the Saran and the clods divided into two groups. One group was immediately submerged in 0.01 M solutions for 15 days for a second time. Another set of clods was evacuated overnight in a desiccator prior to submersion in 0.01 M solutions which were introduced through a two-way stopcock in the desiccator. Final volumes were

determined as previously. Specific volumes of the clods at various stages in the experiment were calculated and expressed on a 105°C-dry basis. Each clod treatment was done in triplicate.

Quantities of exchangeable ions occurring in each soil were determined on air-dried samples prior to any treatments and on clods following their final equilibration in the 0.01 M ionic strength solutions. Exchangeable basic cations were determined by atomic adsorption analysis of 1 N ammonium acetate extracts. Exchangeable acidity (taken as trivalent Al) was determined by titration of 1 N KCl extracts.

Mean crystal separation distances of expansive 2:1 phyllosilicates (D_I) were evaluated from XRD patterns as:

$$D_I = \frac{\sum_i (d(001)_i - 9.6)C_i}{\sum_i C_i} \qquad [42]$$

where $d(001)_i$ is the diffraction spacing arising from the (001) plane of MT or VR in Å and C_i is the corresponding diffraction intensity. The XRD patterns were obtained from DCB-treated clay fractions sedimented onto millipore filters and leached with 0.01 M solutions of the same composition used for clod immersion. After transferring to glass slides, the samples were x-rayed while wet, after air-drying and again after re-wetting.

N_2 adsorption surface areas of freeze-dried and air-dried undisturbed soil and of CL, CO, and CH compacted samples were determined in the same manner as in Experiments 1 and 2.

RESULTS AND DISCUSSION

Experiment 1

Effects of compaction

Nitrogen desorption pore size distributions of Ca-montmorillonite samples prior to wetting are shown in Figure 5. A gradual increase in the fraction of pores $<10^3$ Å is evident as density increases from 0.52 to 1.37 g/cm^3 followed by a dramatic increase for the highest density sample. Mercury intrusion analyses on the 0.52 and 1.06 g/cm^3 samples agreed with N_2 data within a few percent for the volume of pores $<10^3$ Å and indicated that the volume of pores $<10^4$ Å was 79 and 98%, respectively.

Dry static compaction had little effect on N_2 BET surface areas. Initial samples of density 0.52 to 1.37 g/cm^3 had N_2 surface areas of 21 to 23 m^2/g. The ratio of total surface area to N_2 surface area suggests a statistical crystalline thickness of 35 to 39 platelets. Compaction to 1.59 g/cm^3 increased the N_2 surface area to 28 m^2/g, indicating a disruption of structural units due perhaps to intracrystalline shear. Pressures generated during wetting apparently reversed this process, since final N_2 surface areas for all treatments were 20 to 22 m^2/g. Final N_2 surface areas were used to calculate osmotic and intracrystalline adsorption.

The measured variations in N_2 surface area resulted in only small differences in predicted osmotic plus intracrystalline adsorption in 0.01 N $CaCl_2$ as a function of initial density. However, as seen in Figure 6, measured water adsorption after submersion varied greatly

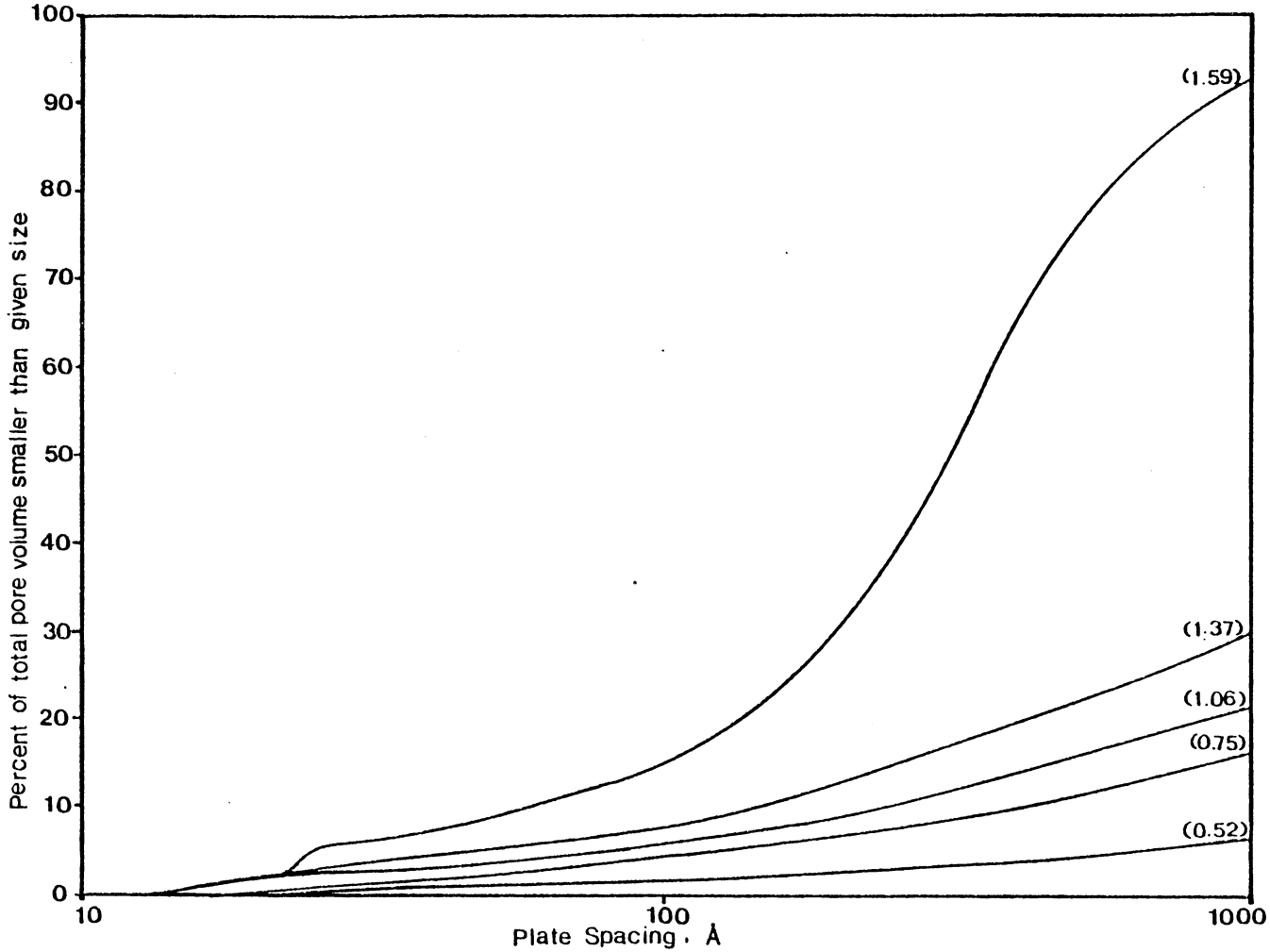

Figure 5. Effects of compaction on N_2 desorption pore size distributions of Ca-MT prior to wetting. Initial densities in g/cm^3 given in parenthese above each curve.

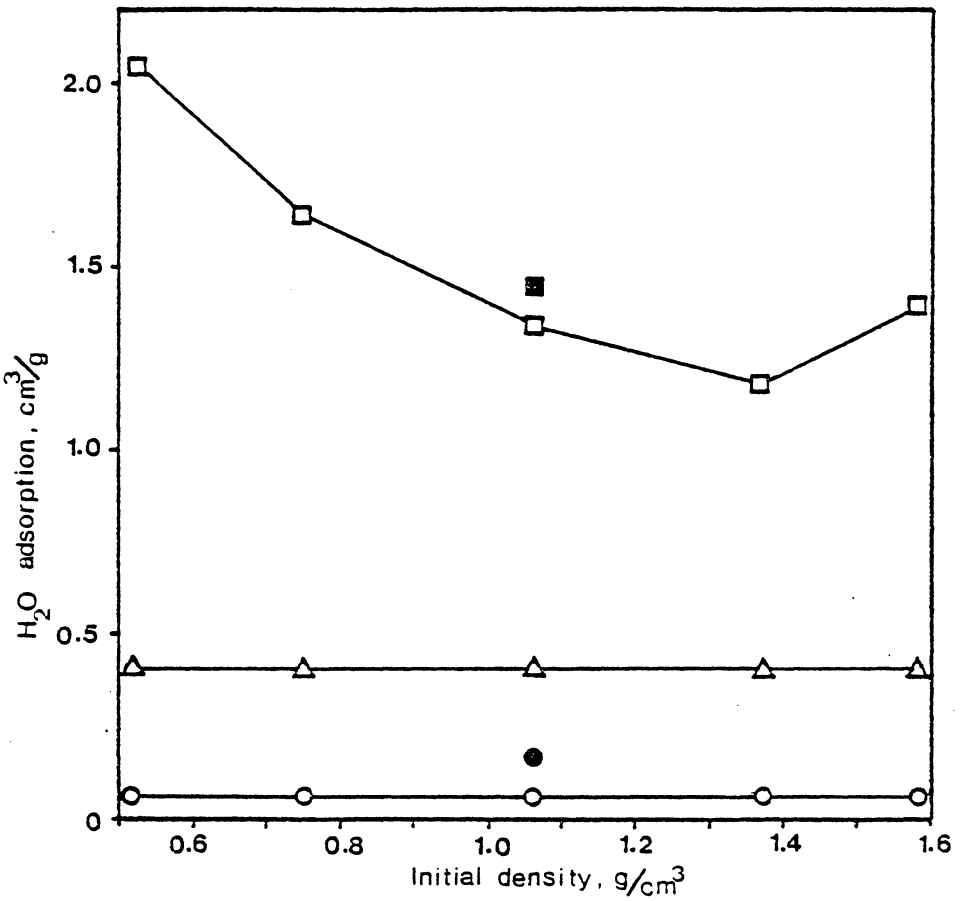

Figure 6. Effects of compaction on water adsorption of P_2O_5-dry cores of Ca-MT. (□) measured total adsorption after submersion in 0.01 N $CaCl_2$; (■) measured total adsorption after sumbersion in 0.001 N $CaCl_2$; (○) predicted osmotic adsorption in 0.01 N $CaCl_2$; (●) predicted osmotic adsorption in 0.001 N $CaCl_2$; (△) predicted intracrystalline adsorption.

with initial density. The difference between measured and predicted adsorption represents the volume of water present external to non-overlapping double layers. The decrease in this "occluded water" as density increased from 0.52 to 1.37 g/cm^3 is readily explained by the observed reduction in the initial volume of pores which exceed double layer dimensions (Figure 5). The increase in "occluded water" for the highest density sample, however, indicates that additional factors must be considered. Evidently, expansion beyond double layer dimensions is occurring.

What could cause this enhanced expansion? On immersion, a wetting front will move inward drawn by capillarity. If air diffusion is limited, gaseous pressures will develop which may induce expansion. The magnitude of these entrapped air pressures should vary inversely with pore size in accordance with the Laplace equation:

$$P = 2\ \gamma_{H_2O}/d \qquad [43]$$

where P is the pressure, γ_{H_2O} is the surface tension of water, and d is the plate separation. The observed reduction in pore size during compaction will then have two opposing effects: (1) a reduction in the initial pore volume exceeding double layer dimensions, and (2) an increase in entrapped air pressures. It is significant that the increase in "occluded water" for the highest density sample (Figure 6) is associated with the most pronounced reduction in pore size (Figure 5).

Estimated intracrystalline and osmotic swelling are shown in Figure 7 along with measured specific volume changes after submersion in 0.01 N $CaCl_2$. Estimated expansion remained virtually constant while

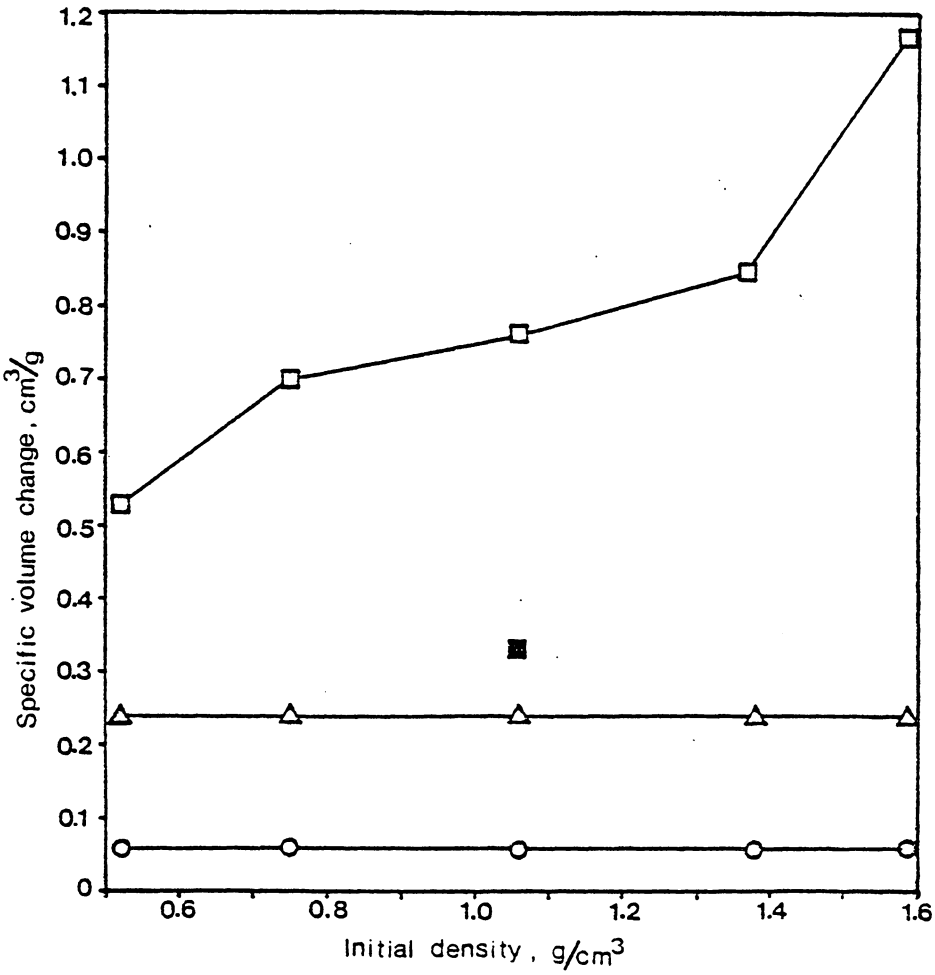

Figure 7. Effects of compaction on expansion of P_2O_5-dry cores of Ca-MT. (□) measured total expansion after submersion in 0.01 N $CaCl_2$; (■) measured total expansion following slow wetting with 0.01 N $CaCl_2$ preceded by vapor wetting; (○) estimated osmotic swelling in 0.01 N $CaCl_2$; (△) estimated intracrystalline swelling.

measured expansion increased continuously with increasing initial density. These increases in expansion closely follow the observed reductions in pore size (Figure 5) which according to Equation 43 should cause an increase in entrapped air pressures. The greatest increase in expansion is observed to occur between 1.37 and 1.59 g/cm^3 density, corresponding to the most marked reduction in initial pore size. Roughly 50 to 75% of the total expansion following submersion in 0.01 N $CaCl_2$ appears to be attributable to swelling caused by entrapped air pressures depending on initial density. Of the remainder, about 75% is estimated to be due to intracrystalline swelling and about 25% to osmotic swelling (Figure 7).

Effects of electrolyte

Reducing the concentration of $CaCl_2$ from 0.01 to 0.001 N should increase osmotic adsorption by 0.11 cm^3/g as double layer thickness increases from $\sim$ 30 to 83 Å, but it should have no effect on intracrystalline adsorption. Measured total adsorption was found to be 1.34 and 1.45 cm^3/g for submersion of 1.06 g/cm^3 initial density samples in 0.01 and 0.001 N $CaCl_2$, respectively. Their respective specific volume changes were 0.77 and 0.88 cm^3/g. These increases in water adsorption and expansion caused by reducing electrolyte concentration are equal to the predicted increase in osmotic adsorption. The existance of an osmotic component to water adsorption and swelling appears to be confirmed.

Double layer theory does not predict a difference in H_2O adsorption for surfaces in contact with $CaCl_2$ or $Ca(H_2PO_4)$ solutions of the

same concentration. Measured specific expansion and water adsorption, however, increased by 0.15 cm^3/g when 1.06 g/cm^3 initial density samples were submerged in 0.01 N $Ca(H_2PO_4)_2$ rather than 0.01 N $CaCl_2$. Adsorption of phosphate on mineral edges would be expected to reduce Coulombic edge-to-face interactions. The importance of edge-to-face bonds in limiting expansion has been noted by other authors (Norrish et al., 1963; Rowell, 1965).

Effects of rate of wetting

Vapor H_2O adsorption by the 1.06 g/cm^3 initial density sample began to plateau at a water content of 0.30 g/g and a specific volume change of 0.17 cm^3/g. Following gradual wetting with 0.01 N $CaCl_2$, water adsorption increased to 0.90 cm^3/g resulting in an additional 0.20 cm^3/g expansion. Total expansion was thus reduced from 0.77 cm^3/g for immediate submersion in 0.01 N $CaCl_2$ to 0.33 cm^3/g for the slow wetting procedure. The estimated intracrystalline plus osmotic swelling was 0.30 cm^3/g. This leaves only 0.03 cm^3/g expansion unaccounted for during slow wetting as opposed to 0.47 cm^3/g during rapid wetting.

The close agreement between estimated and measured swelling for slow wetting may be merely fortuitous, but the dramatic effect of rate of wetting appears to confirm the importance of swelling caused by entrapped air. During wetting from the vapor state no capillary pressures will develop in response to the advance of a wetting front, because no true wetting front exists. The gradual addition of liquid water or dilute electrolyte favors the dissipation of entrapped air pressures because of the localized nature of the wetting front. Thus,

swelling due to entrapped air is greatly reduced during slow wetting. This interpretation is supported by results given by Emerson (1964) who reported that sample evacuation prior to submersion also reduced swelling.

The foregoing scenario is supported by the changes in pore size distribution observed following slow and fast wetting given in Table 1. Slow wetting produced a 0.28 cm^3/g increase in the volume of 10^3 to 10^4 Å pores and a 0.08 cm^3/g increase in $>10^4$ Å pores, while rapid wetting resulted in a 0.14 cm^3/g decrease in 10^3 to 10^4 Å pores and a 1.17 cm^3/g increase in $>10^4$ Å pores. This pronounced expansion of 10^3 to 10^4 Å pores during rapid wetting cannot be accounted for by the extension of double layers which are less than 100 Å in thickness.

Table 1. Pore size distributions of 1.06 g/cm^3 initial density samples by Hg intrusion before wetting and after slow and fast wetting.

Sample treatment	Pore volumes in cm^3/g for various pore sizes 20-100 Å	10^2-10^3 Å	10^3-10^4 Å	>10^4Å
Before wetting	0.03	0.09	0.35	0.01
After slow wetting	0.03	0.03	0.63	0.09
After fast wetting	0.06	0.02	0.21	1.18

Experiment 2

The values of c-axis spacings for the different clays when wet, air-dry, and oven-dry, and N_2 adsorption surface areas of the compacted clays are given in Table 2. Calculated double layer thicknesses in 0.01 N NaCl, $CaCl_2$, and $AlCl_3$ were 35.0, 29.5, and 26.3 Å, respectively. Predicted intracrystalline and osmotic components of water adsorption and expansion calculated from the data in Table 2 and theoretical double layer thicknesses are presented in Figures 8 and 9.

Predicted intracrystalline adsorption decreased in the order: Al-MT > Ca-MT > Na-VR ≈ Ca-VR ≈ Al-VR, largely reflecting differences in wet c-axis spacings of the different clays. Predicted intracrystalline expansion values (Figure 9) which follow the order: Al-MT > Ca-MT > Na-VR > Al-VR ≈ Ca-VR, reflect the magnitude of c-axis spacing increases from air-dry to wet conditions. Because of the rather large differences between total and N_2 surface areas, predicted osmotic adsorption was substantially lower than intracrystalline adsorption for all samples--except, of course, for Na-MT which was assumed to form diffuse double layers on all surfaces.

Vapor adsorption and expansion

The results of water adsorption and expansion measurements following vapor wetting are given in Figures 8 and 9. Measured vapor adsorption followed the order: Na-MT > Al-MT > Ca-MT > Ca-VR > Na-VR > Al-VR. Measured expansion followed the sequence: Na-MT > Al-MT > Ca-MT > Na-VR > Ca-VR > Al-VR. With the exception of the Na-MT sample, there

Table 2. C-axis spacings of wet, air-dry, and 105°C-dry clay, and N_2 surface areas of compacted samples.

Clay	C-axis spacings			N_2 surface area
	Wet	Air-dry*	105°C-dry	
	Å			m^2/g
Na-MT	---	11.9	9.6	22
Ca-MT	19.4	15.0	10.8	20
Al-MT	22.3	13.9	12.4	27
Na-VR	14.6	12.2	9.8	31
Ca-VR	15.0	14.6	11.9	35
Al-VR	14.6	13.9	12.4	40

* Relative humidity = 27% at 22°C.

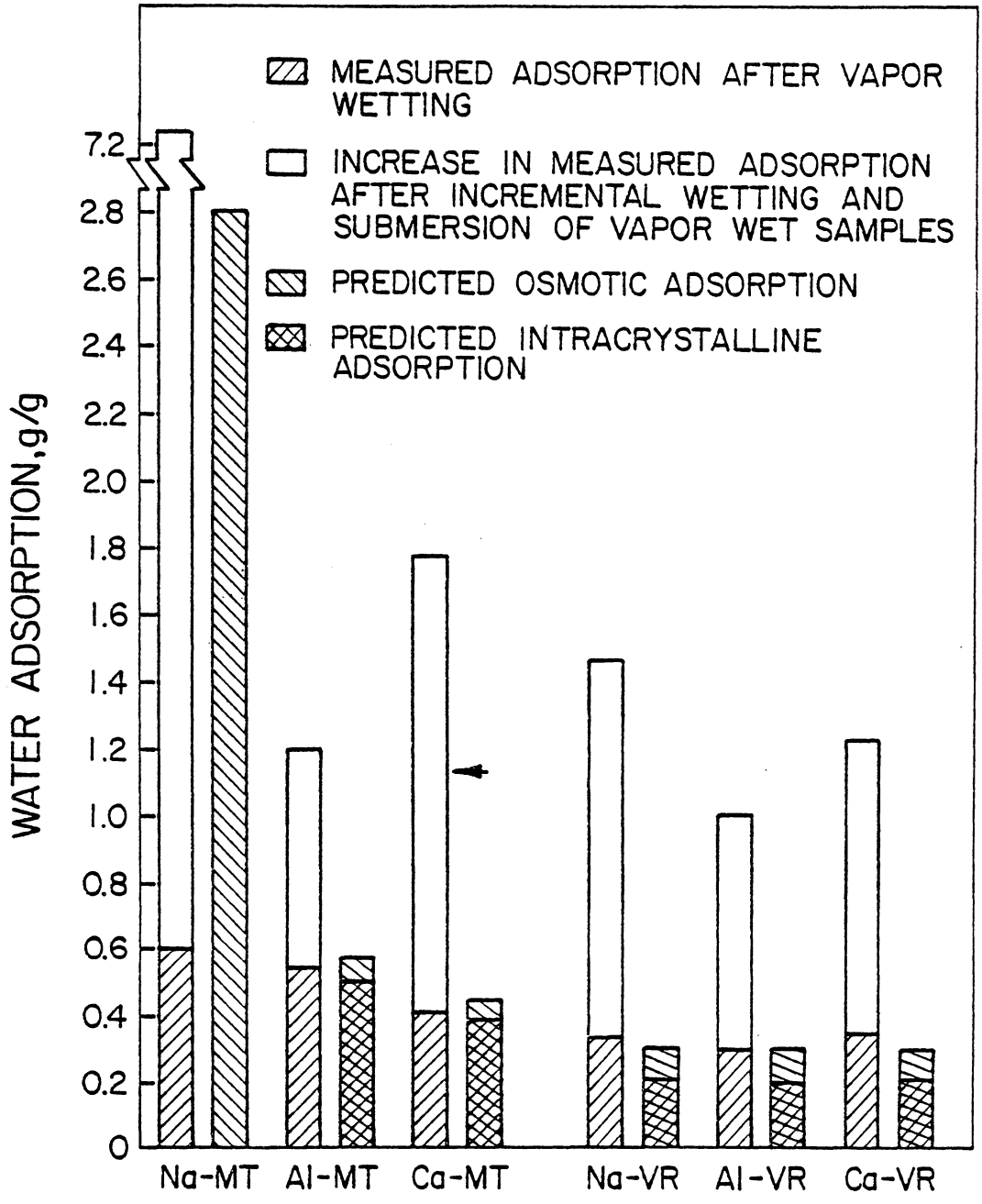

Figure 8. Measured adsorption after vapor wetting and subsequent submersion in 0.01 N electrolyte and values of predicted osmotic and intracrystalline adsorption. Arrow indicates measured adsorption for vacuum-wet Ca-MT.

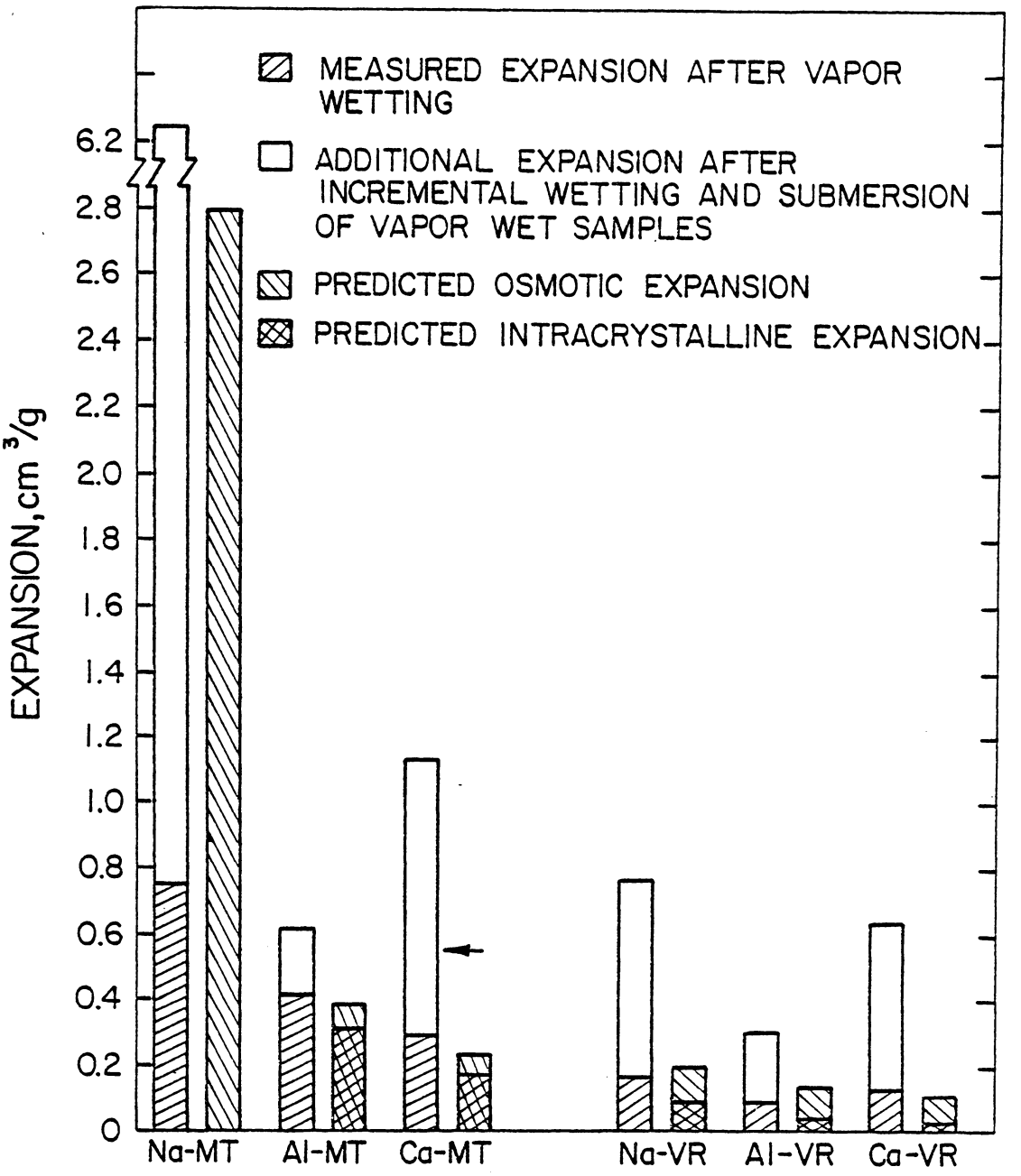

Figure 9. Measured expansion after vapor wetting and subsequent submersion in 0.01 N electrolyte and values of estimated osmotic and intracrystalline expansion. Arrow indicates measured expansion for vacuum-wet Ca-MT.

appears to be an approximate correspondence between measured vapor adsorption and predicted intracrystalline plus osmotic adsorption, as well as between measured and predicted expansion. This correspondence, however, should be considered somewhat fortuitous, since the magnitude of osmotic adsorption is indeterminant for at least two reasons. First, the residual salt contents and hence the equilibrium electrolyte concentrations are not known. Second, it is unlikely that diffuse double layer formation is possible for adsorption from vapor. As with all diffusion processes, diffuse double layer formation is essentially an entropic phenomena. Because the entropy of gaseous water is greater than that of liquid water, it seems probable that double layer formation will be restricted by vapor adsorption.

Although osmotic adsorption is indeterminate following equilibration with saturated water vapor, intracrystalline adsorption should be complete (Emerson, 1962a; Keren and Shainberg, 1975). A comparison of predicted intracrystalline adsorption with measured vapor adsorption reveals a small difference between the two values for Ca- and Al-montmorillonite but a considerable disparity for all the vermiculite samples. Similar comparisons between measured expansion following vapor wetting and predicted intracrystalline expansion indicate that all expansion is not accounted for by intracrystalline volume changes. However, intracrystalline expansion appears to account for a significant portion of swelling, particularly for Al-MT and Ca-MT. The general trend in expansion for vapor wetting parallels the magnitude of intracrystalline adsorption, with Al-MT the greatest, followed by Ca-MT, and in turn by the vermiculites.

In order to further investigate the relationships between water adsorption and expansion, let us compare measured expansion for vapor wetting with measured moisture content changes. Since initial moisture contents were less than required to completely fill the initial interlayer spaces, a volume of water equal to the difference between initial intracrystalline volume and initial water content will have no effect on expansion. Initial intracrystalline volume may be estimated as one half the product of internal surface area and air-dry plate spacing. Taking the ratios of measured volume change to the difference between vapor adsorption and initial intracrystalline volume, we find values of 1.47, 1.45, and 1.13 for Na-MT, Ca-MT, and Al-MT, and 0.71, 0.87, and 0.69 for Na-VR, Ca-VR, and Al-VR, respectively. Thus, after filling the initial intracrystalline spaces, water adsorption resulted in a superequivalent volume change for the montmorillonites and a subequivalent volume change for the vermiculites.

In the vermiculites, part of the water adsorbed is apparently accommodated within relatively large pores in the system without effecting any expansion. Water adsorption in the montmorillonites, however, apparently induces distortions or rearrangements of crystals which, in turn, cause expansion in excess of the volume of water adsorbed. To evaluate differences in microstructure of montmorillonite and vermiculite which might account for this behavior, we may compare the morphology of the samples revealed in the scanning electron micrographs shown in Figure 10. The morphology of the vermiculites varies little with ion saturation and is comprised of irregularly shaped crystals which exhibit very little bending in the c-dimension. The montmorillonites,

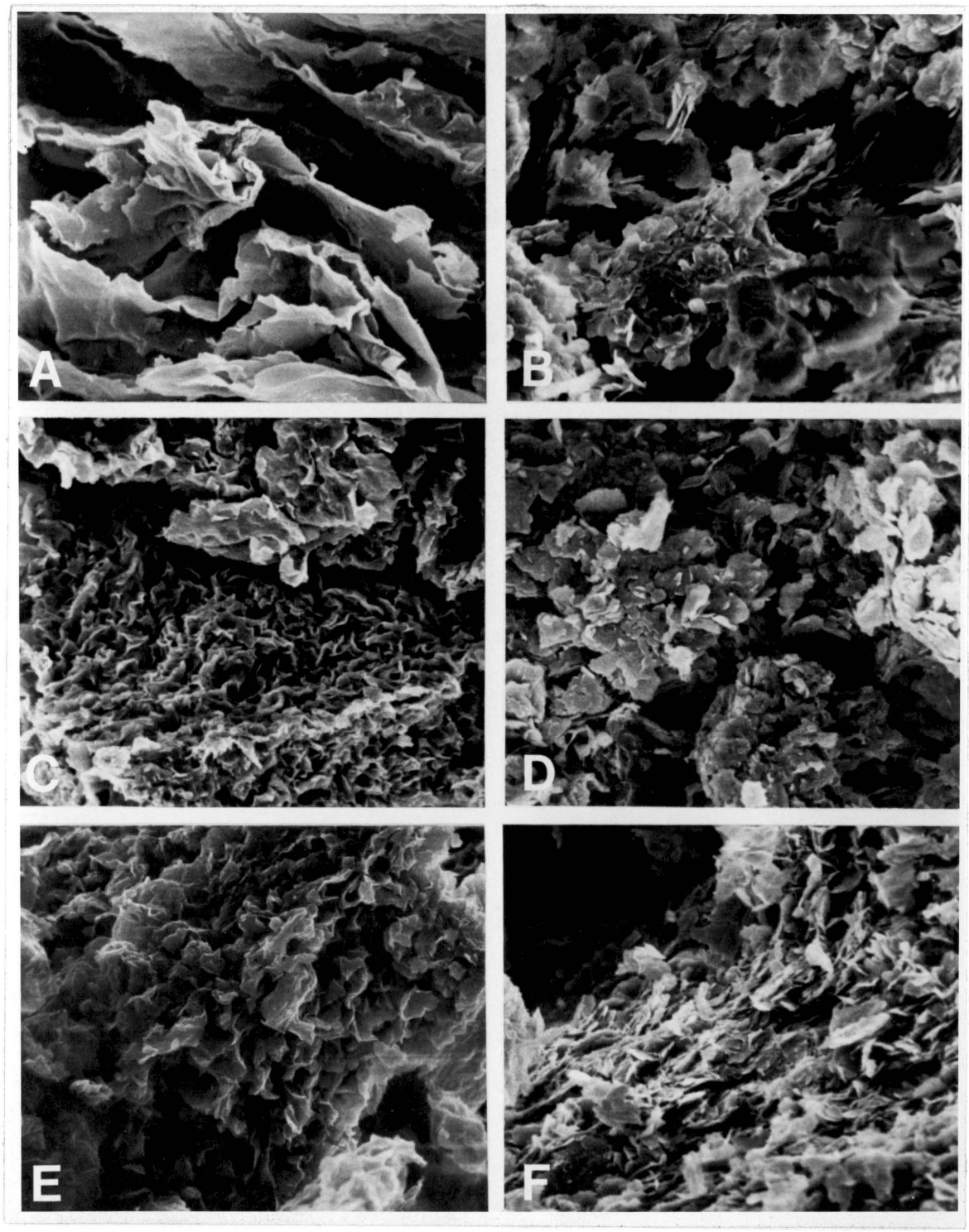

Figure 10. Scanning electron micrographs of compacted clays prior to wetting. 2000 X. (A) Na-MT, (B) Na-VR, (C) Ca-MT, (D) Ca-VR, (E) Al-MT, (F) Al-VR.

on the other hand, all show some degree of c-axis distortion which decreases in the order Na-MT > Ca-MT > Al-MT. A qualitative relationship between degree of particle distortion and the calculated swelling to adsorption ratios suggests that relaxation of strained crystals during wetting may contribute significantly to clay swelling.

Adsorption and expansion after submersion

Following incremental wetting and submersion of vapor-wet samples in 0.01 N salt solutions, water adsorption and expansion increased markedly (Figures 8 and 9). A large difference between vapor and liquid phase water adsorption and expansion has also been observed by Emerson (1962a,b) for Ca-MT. The increase in adsorption and swelling during liquid phase wetting could not be attributed to intracrystalline adsorption which was complete after equilibration at a relative vapor pressure of 0.985. An inverse relationship between electrolyte concentration and liquid phase adsorption and associated swelling suggested osmotic forces were responsible for the increase in adsorption and swelling. As we have already mentioned, an increase in osmotic adsorption may be expected because of the difference in entropy of vapor and liquid phase water.

However, we see in this study that the increase in adsorption following submersion greatly exceeds predicted osmotic adsorption. This in itself could simply indicate a large amount of water held by capillary forces in pores exceeding double layer dimensions, yet we also observe a large disparity between predicted osmotic adsorption or expansion and the increase in expansion accompanying liquid phase wetting. It is possible that osmotic adsorption is being underestimated

if the surface areas subject to diffuse double layer formation exceed N_2 surface areas. Such an eventuality has been suggested by Homshaw and Chaussidon (1979). However, the magnitude of the discrepancy between measured and predicted expansion suggests that this is not the sole explanation and that other mechanisms are probably involved in swelling.

Quirk (1978) has suggested that expansion may result from shearing between randomly arrayed "domains" caused by their swelling in different directions. In this way a relatively small "intradomain" expansion could be magnified at the macroscopic level. Restriction of the rotational and translational movements of these structural units would greatly inhibit expansion. The observed increases in expansion following incremental wetting and submersion of the vapor-wet samples decreased in the order: Na-MT >> Ca-MT > Al-MT for the montmorillonites and Na-VR > Ca-VR > Al-VR for the vermiculites. Thus, for both minerals, expansion decreased with increasing counterion valence. With increasing ion valence, we may expect net attraction at particle contacts to increase. This may arise through cation bridging between planar surface contacts or through increasing edge-to-face bonds due to specific adsorption of multivalent cations on the mineral edges (McBride, 1978; Parker et al., 1979). The importance of edge-to-face bonds in diminishing swelling was verified in Experiment 1.

At the lowest structural level, expansion may be associated with osmotic adsorption to some degree. It also seems possible that the relaxation of distorted crystals accompanying a reduction in capillary cohesion during submersion may contribute to expansion at the microscopic and ultimately at the macroscopic level. The results of

Experiment 1 suggested that rapid wetting could induce pressures in air trapped ahead of an advancing wetting front, resulting in sample expansion. Gradual wetting was found to greatly diminish this effect--slow wetting reduced water adsorption of 1.06 g/cm^3-compacted Ca-MT from 1.34 g/g for rapid submersion in 0.01 N $CaCl_2$ to 0.90 g/g. However, we observe in the present experiment that final water adsorption by Ca-MT compacted to a similar initial density and subjected to slow wetting (vapor adsorption-incremental wetting-submersion) was 1.82 g/g in 0.01 N $CaCl_2$. This is twice the value found by the same wetting procedure in Experiment 1. Evacuation prior to submersion of Ca-MT in the present experiment reduced the final water content by 36% and expansion by 51% (Figures 8 and 9). Thus, the Ca-MT in this experiment appears to exhibit greater expansion due to entrapped air pressures even during slow wetting. What is responsible for this difference in behavior?

Sample preparation of the clays in the two experiments differed in one major respect--in Experiment 1, the clay was oven-dried prior to compaction, while in the present experiment it was freeze-dried. The total porosities of the oven-dried and freeze-dried Ca-MT prior to compaction differed markedly--the former having a pore volume of about 1.85 cm^3/g and the latter about 6.30 cm^3/g. This apparent difference in particle arrangement was not reflected in N_2 surface areas which were similar for the two samples after compaction.

According to Equation 43, entrapped air pressures should increase with decreasing pore size. To see if this could account for the effects of preparation method on the swelling of Ca-MT, pore size distributions of freeze-dried and oven-dried Ca-MT compacted to 0.98

and 1.06 g/cm^3 density, respectively, were measured by Hg intrusion as in Experiment 1. The results, shown in Table 3, are unfortunately ambiguous. Judging from the intruded volumes, the freeze-dried clay appears to have fewer small pores than the oven-dried clay. However, a large discrepancy between theoretical total and intruded porosity for the freeze-dried clay suggests that the sample may have compressed during intrusion. Though uncertain, it does not appear that differences in pore size between the freeze-dried and oven-dried clays are responsible for their markedly distinct behavior. Scanning electron micrographs of the two compacted clays prior to wetting were taken to identify morphological differences (Figure 11). Greater crystal distortion is evident in the freeze-dried, compacted Ca-MT, suggesting that the higher swelling exhibited by the freeze-dried clay and its greater susceptibility to expansion by entrapped air pressures may be due to greater strain relaxation during wetting.

It is interesting to conjecture whether crystal bending in the c-plane may be responsible for b-dimension variations observed by Low, Ravina and White (1970) and Ravina and Low (1977). If so, crystal strain relaxation rather than clay-water epitaxy (op. cit.) may be the mechanism governing the relationship between b-dimension and swelling. Ravina and Low (1977) reported differences in b-dimensions of montmorillonites saturated with different cations. To see whether the morphological differences between freeze-dried and oven-dried Ca-MT would be reflected in crystal dimension changes, b-dimensions were measured in duplicate on random powder mounts of uncompacted samples of the two clays by XRD using Cu Kα radiation. Quartz powder was

Table 3. Pore size distributions by Hg intrusion of freeze-dried and oven-dried Ca-MT compacted to 0.98 and 1.06 g/cm^3 densities, respectively.

Sample	Intruded volumes for various pore sizes				Apparent nonintruded volume
	20-100 Å	10^2-10^3 Å	10^3-10^4 Å	>10^4 Å	
	cm^3/g				
Freeze-dried	.03	.04	.04	.35	.18
Oven-dried	.03	.08	.36	.08	.02

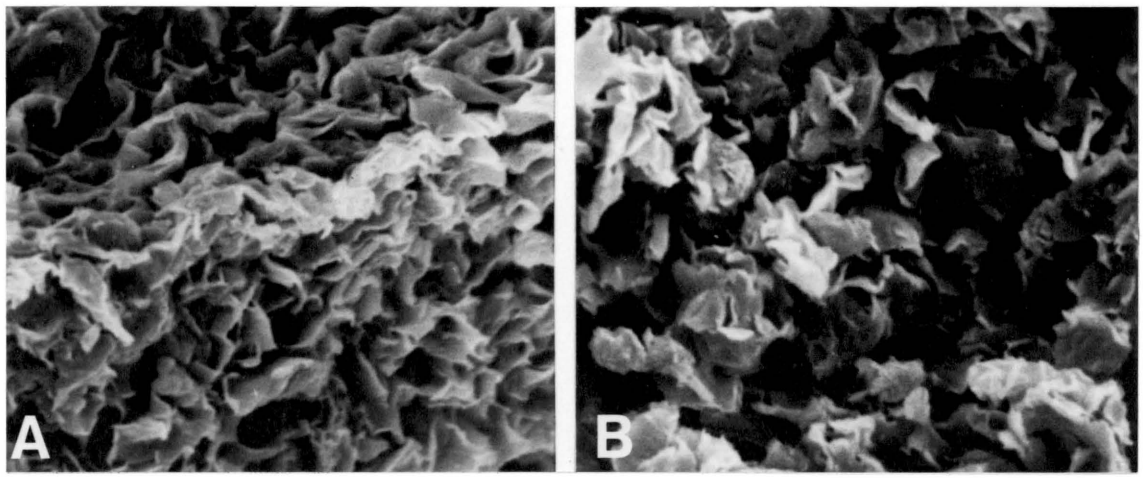

Figure 11. Scanning electron micrographs of (A) freeze-dried, and (B) oven-dried, compacted Ca-MT prior to wetting. 5000 X.

mixed with the clays and the quartz (113) diffraction maximum, taken as 1.543 Å, was used as an internal standard. The (060) diffraction maxima of the clays were quite broad, indicating a wide range in b-dimension for each sample as would be expected for highly strained crystals. Accordingly, the peak width was greater for the freeze-dried clay than the oven-dried clay. For the oven-dried clay, 50% of the peak area occurred over 0.36°2θ, while for the freeze-dried clay the analogous figure was 0.47°2θ, corresponding to ranges in b-dimension of 0.050 and 0.062 Å, respectively. Mean b-dimensions corresponding to the mid-points of the peak areas were 8.993 Å for the oven-dried clay and 8.990 Å for the freeze-dried clay--the average difference between duplicates being only ± 0.0005 Å. It appears that the b-dimension of montmorillonite is indeed related to crystal strain in the c-plane.

Experiment 3

Characterization of samples

Particle size distribution and mineralogical composition of the soils in this experiment are presented in Table 4. On a whole soil basis, montmorillonite comprises about 9% of the Poplimento soil and 48% of the Iredell, while vermiculite comprises about 11% and 15%, respectively. Surface areas of non-expansive mineral fractions (S_o) calculated from the data in Table 4 by employing Equation 37 are 3.4 m^2/g for Poplimento and 0.8 m^2/g for Iredell. Theoretical total surface areas of the soils calculated from Equation 39 are 163 and 505 m^2/g, respectively, for Poplimento and Iredell.

Compositions of the exchange complexes of the two soils are shown in Table 5 for samples before and after equilibration with the 0.01 M ionic strength solutions used to immerse clods (see Appendix). Selectivity for K is indicated by the increases in exchangeable K following equilibration with these solutions. Calculated Ca-K Gapon coefficients are 4.0 for Poplimento and 1.2 for Iredell. This K selectivity may be attributed largely to the vermiculite present in the soils which probably has some degree of hydroxy-Al interlayer development. The occurrence of interlayers is supported by XRD data and by the low effective exchange capacities of montmorillonite and vermiculite in the soils estimated from mineralogy and CEC data to be less than about 50 meq/100 g.

Maximum compacted densities of the Poplimento and Iredell samples were 1.40 and 1.38 g/cm^3, achieved at moisture contents of 290 and

Table 4. Particle size distributions and mineralogy of the silt and clay fractions and whole soils.

Soil	Fraction*	Mineral Components*, %						
		MT	VR	KK	MI	QZ	Other	DCB Fe
Poplimento	Clay (45%)	20	25	11	24	15	nd	---
	Silt (48%)	nd	nd	7	10	75	8	---
	Whole soil	9	11	--	--	--	--	3.7
Iredell	Clay (67%)	70	19	6	nd	5	nd	---
	Silt (17%)	5	15	3	9	60	8	---
	Whole soil	48	15	--	--	--	--	2.6

* Values in parentheses are weight percentages of size fractions; remainder from 100% for each soil is sand. Sand = 50-2000 μm, silt = 2-50 μm, clay = <2μm.

* MT = montmorillonite (some hydroxy-Al interlayering), VR = vermiculite (some hydroxy-Al interlayering), KK = kaolinite, MI = mica, QZ = quartz; nd = none detected; — = not evaluated.

Table 5. Exchangeable cations in soils before and after equilibration with 0.01 M ionic strength "soil solutions" calculated assuming Gapon coefficients of 1.0.

Sample	Exchangeable ions, meq/100g					
	Na	K	Ca	Mg	Al*	Total
Poplimento - initial	0.07	0.16	3.49	1.60	0.65	5.97
Poplimento - final	0.08	0.70	3.91	1.50	0.55	6.74
Iredell - initial	0.40	0.30	11.10	17.00	0.45	29.25
Iredell - final	0.40	0.45	13.50	25.00	0.15	39.50

* Equivalents of acidity titrated in 1 N KCl extracts.

340 mg/g, respectively. Moisture contents corresponding to 90% of maximum density, below and above optimum moisture, respectively, were 190 and 395 mg/g for Poplimento and 240 and 430 mg/g for Iredell. Moisture contents of replicate compacted clods were within ± 4 mg/g and densities were ± 0.01 g/cm^3. Undisturbed Poplimento samples had initial densities of 1.37 ± 0.04 g/cm^3 and moisture contents of 269 ± 7 mg/g, while Iredell clods were 1.47 ± 0.03 g/cm^3 at 297 ± 2 mg/g.

Effects of compaction on structure

Differences in structure are expected to occur when soil is compacted at various moisture contents. As moisture content increases, interparticle shear resistance decreases, resulting in a reduction in pore size. This reduction in modal pore size may continue above optimum moisture, even though further reduction in total porosity is restricted by the incompressibility of the fluid-filled pores. Differences in pore size may affect the magnitude of entrapped air pressures and associated swelling, as well as the degree to which microscale expansion is absorbed within large pores or manifested macroscopically.

Blackmore and Miller (1961) reported increases in crystal size of Ca-MT caused by preconsolidation. To evaluate the effects of compaction on crystal size, the number of platelets per crystal of MT and VR (n) was calculated as:

$$n = (S_E + S_I)/S_E$$
$$= (S_T - S_O)/(S_{N2} - S_O) \qquad [44].$$

Table 6. Nitrogen adsorption surface areas and calculated average number of platelets per crystal for expansive 2:1 phyllosilicates for various treatments of soils.

Soil	Sample conditions	Nitrogen surface area	Average Platelets per crystal
		m^2/g	
Poplimento	Undisturbed, freeze-dried	39	4.6
	Undisturbed, air-dried and ground	36	4.9
	Compacted* below optimum, freeze-dried	35	5.1
	Compacted at optimum, freeze-dried	34	5.2
	Compacted above optimum, freeze-dried	35	5.1
Iredell	Undisturbed, freeze-dried	65	7.8
	Undisturbed, air-dried and ground	75	6.8
	Compacted below optimum, freeze-dried	79	6.4
	Compacted at optimum, freeze-dried	76	6.7
	Compacted above optimum, freeze-dried	77	6.6

* Compaction carried out on air-dried, ground soil with water added to yield desired moisture content.

Measured N_2 surface areas and calculated values of n for various sample conditions are given in Table 6. Average crystal size of Poplimento increased slightly during air-drying, reflecting enhanced orientation associated with shrinkage. Compaction caused a slight further increase in orientation which peaked at optimum moisture. The Iredell soil, however, exhibited a reduction in average crystal size during air-drying. This disruption of the microstructure might be explained by the tendency observed in Experiment 2 for dehydrated MT crystals to bend and curl in the c-plane. Intracrystalline shearing apparently was also induced during compaction of the Iredell soil, further decreasing the average crystal size.

Effects of compaction on cyclic volume changes

The changes in specific volume of compacted and undisturbed clods during the initial wetting, subsequent air-drying and final re-wetting under atmospheric pressure are shown in Figures 12 and 13 for the Poplimento and Iredell samples.

Poplimento. During the first wetting cycle, expansion will be influenced by differences in initial moisture content, as well as by differences in structure. For samples having the same original structure, potential expansion will diminish with increasing moisture content. The observed relationship between expansion and initial moisture content is shown in Figure 14. It is apparent that the effects of differences in initial moisture content of Poplimento samples have been negated by other factors. Reductions in pore size accompanying increasing compaction moisture contents may be involved.

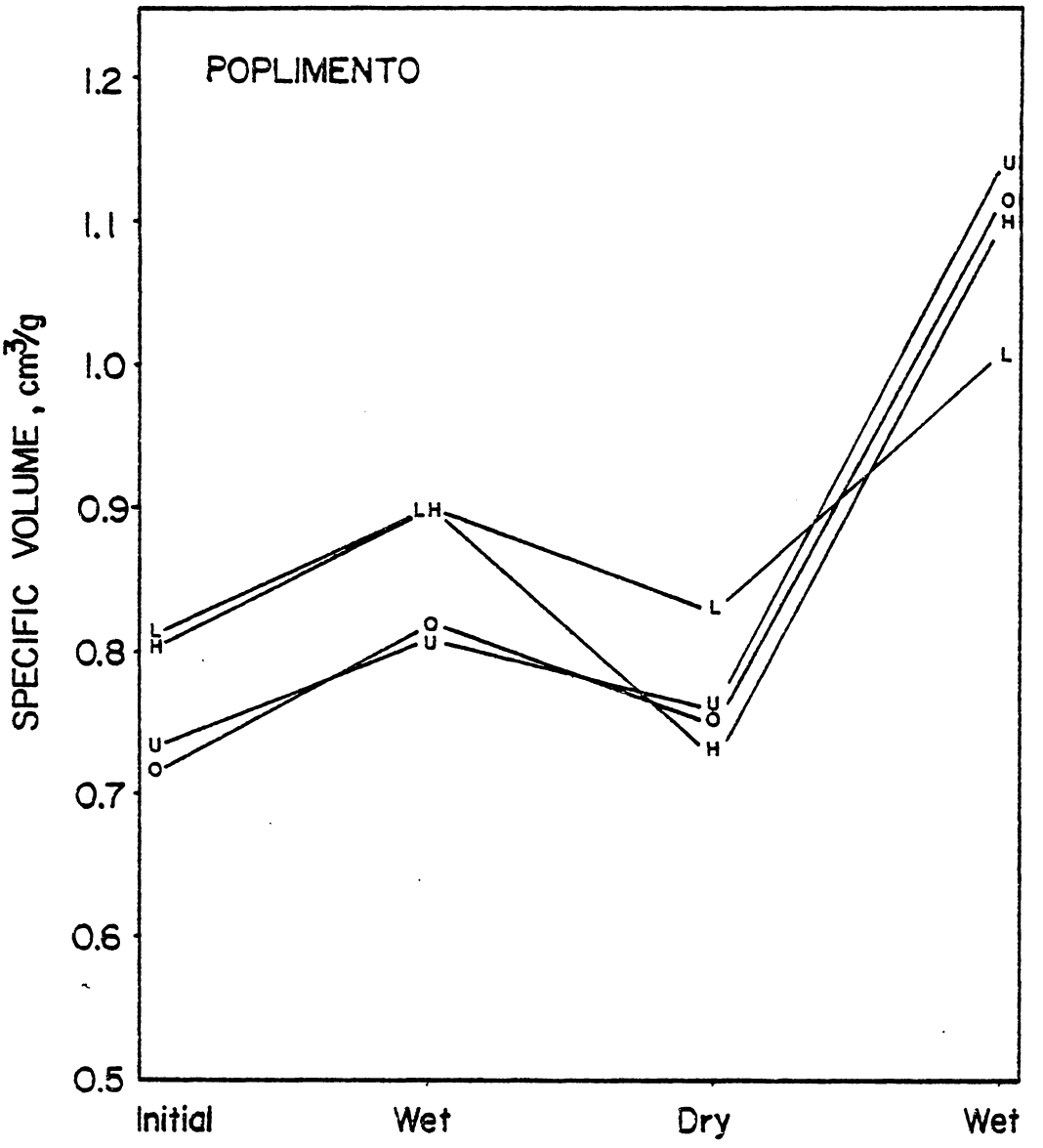

Figure 12. Change in specific volume of Poplimento samples after wetting, air-drying and re-wetting by submersion under atmospheric pressure. Undisturbed samples = U, compacted below optimum = L, compacted at optimum = O, compacted above optimum = H.

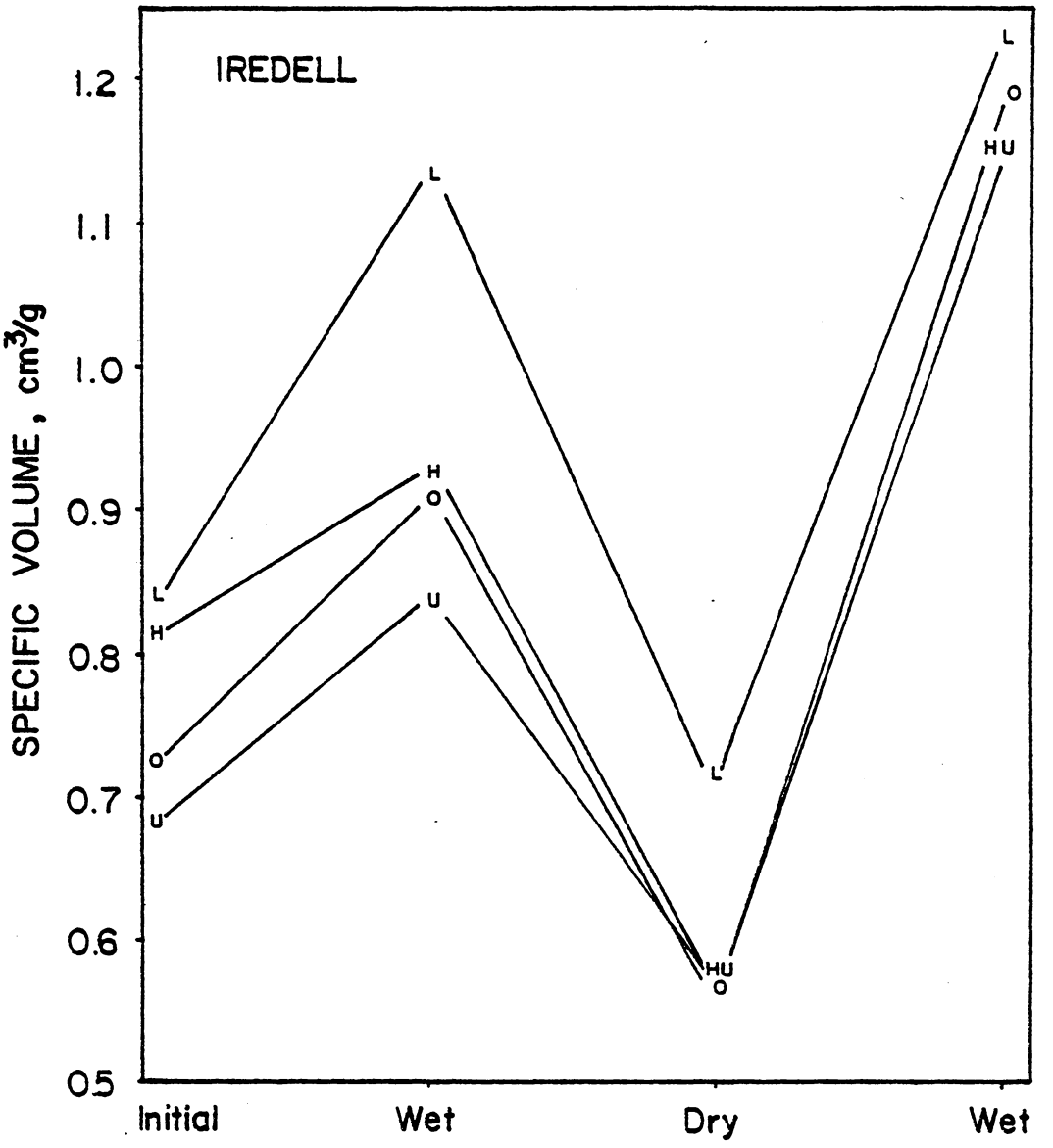

Figure 13. Change in specific volume of Iredell samples after wetting, air-drying and re-wetting by sumbersion under atmospheric pressure. Legend as in Figure 12.

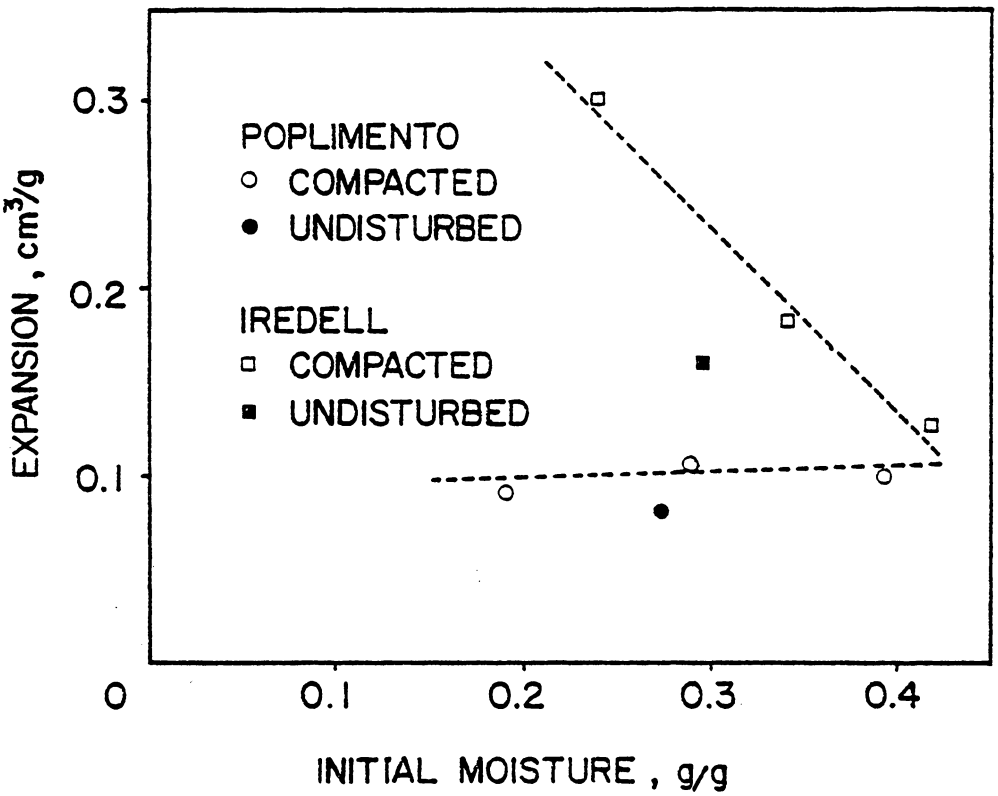

Figure 14. Relationship between initial clod moisture contents and expansion during first wetting cycle.

Smaller pores may, for instance, increase swelling due to entrapped air pressures while also diminishing the accomodation of microscale expansion which would occur in larger pores. Differences in structure associated with compaction at various moisture contents may also affect the magnitude of expansion arising from strain relaxation and differential strains within the clods.

Shrinkage accompanying air-drying was lowest for undisturbed clods, followed closely by CL and CO clods. Much greater shrinkage by CH clods may be attributed to higher initial (wet) total porosities and finer pore size distributions. Finer pores will enhance shrinkage by increasing capillary cohesion. Shrinkage by undisturbed and CO clods is probably limited by their relatively low initial total porosity and greater pore size, while shrinkage of the high porosity CL clods is limited by their coarser pore size distributions.

During the final wetting under atmospheric pressure, the undisturbed, CO and CH clods exhibited similar volume changes, while CL clods underwent much lower expansion. The higher total porosities and coarser pore size distributions of CL clods which limited shrinkage during air-drying apparently persist in the dry samples and limit expansion during re-wetting. Final volumes of all clods were about 10-40% greater after the second wetting than the first, indicating that changes in structure accompanying air-drying have a significant effect on expansion.

Iredell. Unlike the Poplimento samples, expansion of Iredell clods during the first stage of wetting was markedly affected by their initial moisture content. The linear relationship between initial moisture

content and expansion for compacted Iredell samples seen in Figure 14 suggests that differences in structure caused by compaction are of secondary importance to swelling of compacted Iredell soil. Differences in structure between the compacted and undisturbed clods, however, appear to greatly affect expansion. Interpolation between the CH and CO Iredell samples in Figure 14 shows that expansion of soil compacted at a moisture content equal to that of the undisturbed clods would be considerably greater than undisturbed clod swelling. Greater osmotic adsorption resulting from the increase in external crystal surface area accompanying air-drying and compaction will only partially account for this difference in swelling. Other structural changes accompanying drying and compaction, such as increased crystal distortion, are probably involved.

Following air-drying, the undisturbed, CO, and CH clods shrunk to nearly the same density. Although the specific volume change of the CL clods exceeded the other samples, their final specific volumes remained greater than the other treatments. The greater dry specific volume of the CL samples may be due to a larger macropore volume in the form of cracks and fissures resulting from large differential strains during the initial wetting phase. On drying, shrinking may occur within the resulting blocky fragments which remain separated by relatively large voids.

Following rewetting under atmospheric pressure, the densities and specific volume changes of all treatments appear to be converging. However, as was the case with Poplimento, final clod volumes were about 10-40% greater after the second wetting than the first,

indicating again that volume change behavior is greatly influenced by changes in structure accompanying drying.

Components of soil swelling

Measured values of expansion of air-dry soil submerged under atmospheric pressure and under vacuum are shown in Figures 15 and 16, along with predicted values of osmotic and intracrystalline swelling. Internal and external surface areas were calculated using air-dried undisturbed sample values for undisturbed clods and freeze-dried compacted sample values for compacted clods (Table 6). Mean intracrystalline spacings, which were measured on wet, air-dry and re-wet samples, were lower for re-wet than initially wet samples due to the irreversible collapse of certain components--probably K-VR--to approximately 10 Å c-spacings.

Poplimento. Considerable differences occur between atmospheric pressure-wet and vacuum-wet Poplimento clods. These differences, which may be attributed to swelling caused by entrapped air pressures, decrease in the order: undisturbed > CO > CL > CH. Unless pore size follows the unlikely sequence: CH > CL > CO, we are obliged to conclude that swelling due to entrapped air pressures is not simply and directly related to the Laplace pressure given by Equation 43. At least two factors may contribute to this discrepancy. First, the magnitude of the entrapped air pressures may be expected to diminish if the rate of wetting is slow, allowing pressures to dissipate by the diffusion of entrapped air. As hydraulic conductivity diminishes with decreasing pore size, this effect may run counter to the trend indicated by the Laplace equation. A second factor to consider is the resistance of

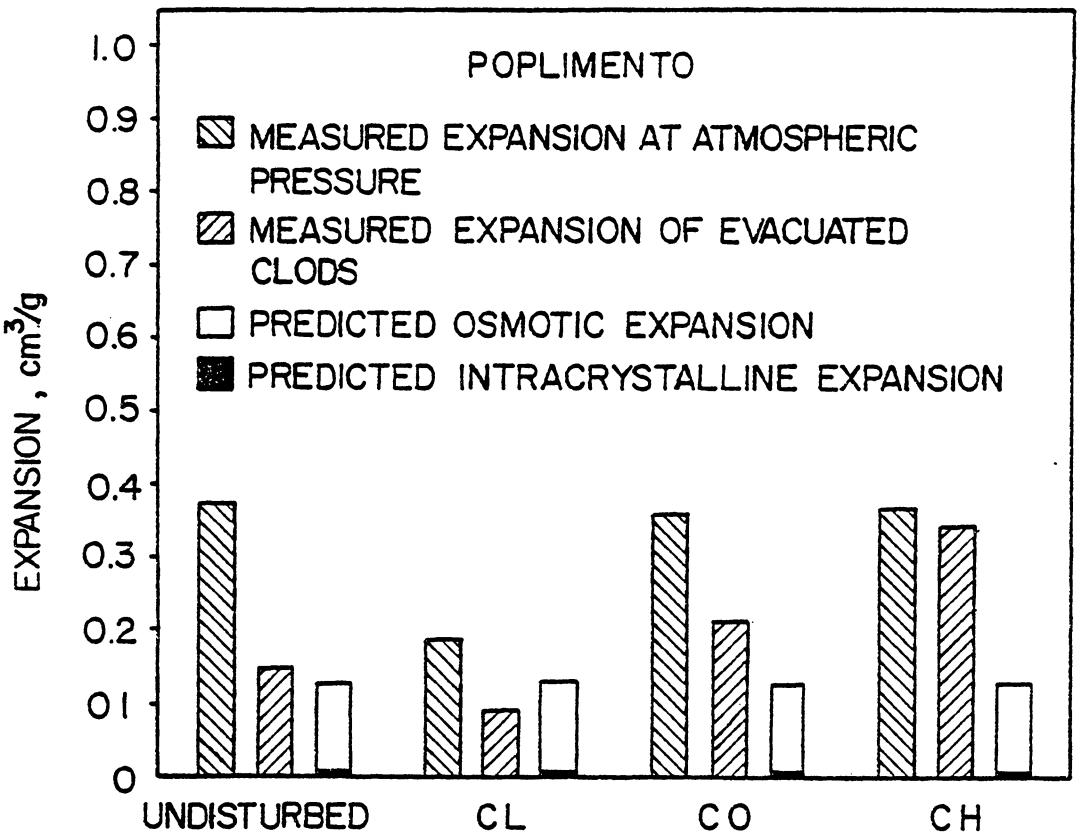

Figure 15. Measured and predicted expansion of Poplimento samples during the final wetting cycle.

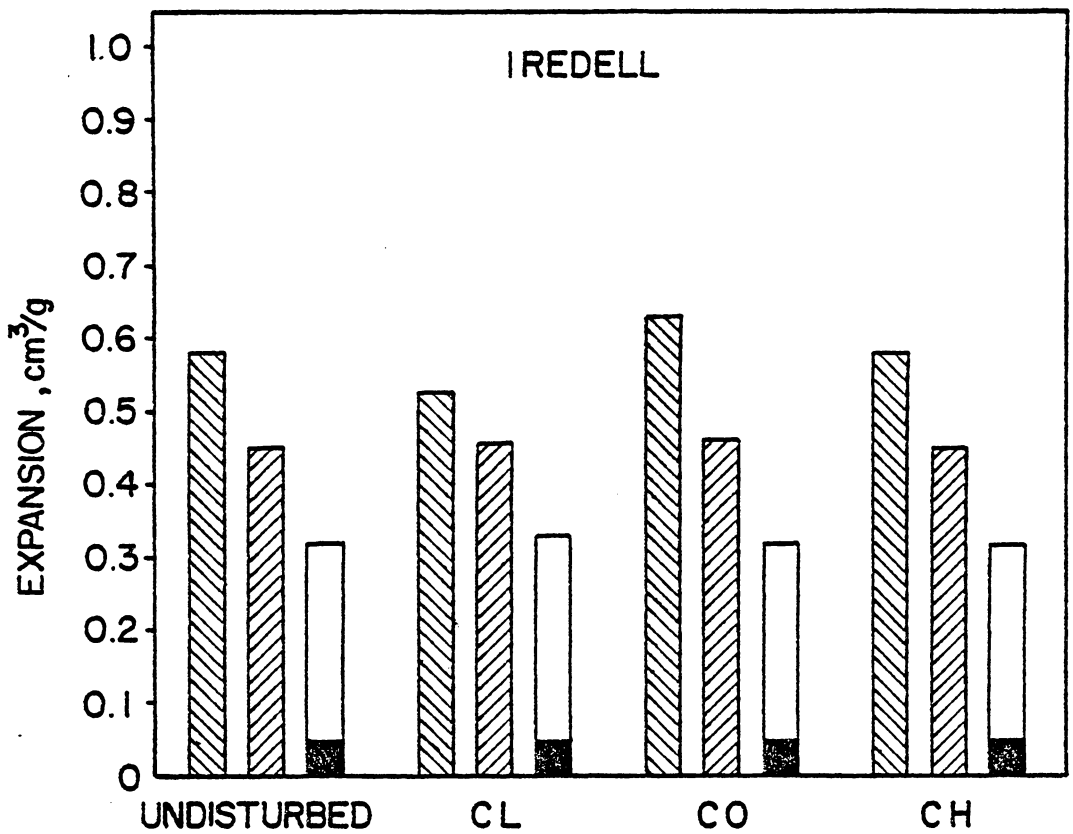

Figure 16. Measured and predicted expansion of Iredell samples during the final wetting cycle. Legend as in Figure 15.

the microstructure to expansion. Even if entrapped air pressures increase with diminished pore size, swelling might be reduced if the resistance to swelling increased due to changes in microstructure--for example, an increase in edge-to-face bonds or greater interleaving of crystals.

Predicted intracrystalline expansion by Poplimento samples was small and nearly equal for all treatments, reflecting the relatively small internal surface areas and changes in mean interlayer spacing. Calculated internal surface areas were approximately 129 m^2/g. Mean d(001) spacings for expansive 2:1 phyllosilicates were 15.4 Å for initially wet, 12.7 for air-dry and 13.7 for re-wet samples, reflecting a considerable amount of irreversible platelet collapse probably due to the high vermiculite content. Even if intracrystalline shrinkage was completely reversible, however, this component of volume change would remain inconsequential.

In contrast to the results of Experiments 1 and 2, predicted osmotic swelling in Poplimento was of considerably greater magnitude than intracrystalline swelling. This discrepancy is largely due to the great difference in crystal size in this and the previous experiments. In the pure MT and VR samples, the average number of platelets per crystal was approximately 20-40, which may be compared with values of approximately 5 in the Poplimento samples (Table 6). Perhaps the high values in the pure systems are a result of orientation during sample preparation caused, for example, by repeated centrifugal acceleration.

Predicted osmotic adsorption is observed to exceed measured vacuum-wet expansion of CL clods, indicating diffuse double layer accommodation

within large pores. Measured vacuum-wet expansion exceeds predicted expansion for the CO and CH clods, the discrepancy being greater for the latter. The difference between vacuum-wet measured and predicted expansion may be taken as the minimum change in volume resulting from strain relaxation and differential strain. The magnitude of these components apparently increases with compaction moisture content indicating differences in structure caused by compaction continue to strongly influence these mechanisms even after a preceding cycle of wetting and drying. Measured vacuum-wet expansion and osmotic adsorption for the undisturbed Poplimento clods are essentially equal. This does not necessarily mean, however, that this is the sole mechanism governing expansion in these samples. It is quite possible that a significant volume of diffuse double layers is accommodated within adjacent large voids and that the remaining expansion is due to strain relaxation or differential strain.

Iredell. The magnitudes of swelling due to entrapped air pressures, evaluated from the differences between atmospheric pressure-wet and vacuum-wet expansion, fall within the same range of values as Poplimento, but in most cases accounted for smaller percentages of total expansion. The values decreased in the order: CO > CH ≃ undisturbed > CL. Again, it is not clear whether differences in pore size distribution alone can account for this variation. Expansion during vacuum-wetting was essentially equal for all samples. Apparently, although differences in structure exist, as evidenced by variations in swelling due to entrapped air pressures, these differences are minimal, or at least of little consequence to swelling during vacuum-wetting.

Predicted intracrystalline swelling for Iredell was greater than for Poplimento due to greater intracrystalline surface areas as well as greater changes in intracrystalline spacing. Calculated internal surface areas were approximately 425-430 m^2/g. Mean d(001) spacings of expansive 2:1 minerals were 17.8 Å for initially wet, 15.1 Å for air-dry, and 17.1 Å for re-wet samples. Due to the lower proportion of VR in Iredell, intracrystalline expansion was more nearly reversible than in Poplimento. Although predicted intracrystalline expansion is greater in Iredell than Poplimento, it nevertheless still comprises a small portion of total measured expansion. Predicted osmotic swelling accounts for a much larger portion of measured swelling--about 60% of vacuum-wet expansion. Again, the high values of predicted osmotic swelling relative to those in Experiments 1 and 2 are due to the comparatively large ratios of external to internal surface area in the soil systems.

A minimum estimate of the contribution of strain relaxation and differential strain to swelling may be estimated from the difference between measured vacuum-wet expansion and predicted expansion. While these components of expansion increased with compaction moisture content for Poplimento, for Iredell their magnitude appeared unaffected by original sample condition following the first stage of wetting and drying. Apparently, structural factors which govern these mechanisms in Iredell are fixed during the process of air-drying. It seems likely that swelling arising from differential strain between crystals and groups of crystals would be sensitive to variations in microstructure which might remain after air-drying. On the other hand, a uniformity in the degree of crystal bending, which would govern the magnitude of

strain relaxation, is more readily visualized to follow air-drying. If this is the case, then it appears that strain relaxation may be a more significant component in the swelling of Iredell than Poplimento. This may be explained by Iredell's much higher content of MT which was seen in Experiment 2 to undergo considerable crystal distortion when dried.

SUMMARY

Experiment 1

Dry static compaction had little effect on predicted osmotic or intracrystalline water adsorption of Ca-MT. In 0.01 N $CaCl_2$, estimated intracrystalline expansion was about four times greater than estimated osmotic expansion, but in 0.001 N $CaCl_2$ it was about one and a half times greater. The existance of an osmotic component to swelling appeared to be confirmed by the observation that the measured increase in swelling caused by decreasing electrolyte concentration was equal to the predicted increase in double layer volume. Edge-to-face bonds were found to significantly reduce expansion.

From about 50 to 75% of the total swelling which followed submersion of Ca-montmorillonite in 0.01 N $CaCl_2$ was attributed to expansion caused by gaseous pressures which develop ahead of advancing wetting fronts. It was suggested that these pressures should increase with decreasing pore size in keeping with the Laplace equation. Accordingly, compaction increased swelling caused by entrapped air pressures as pore size was diminished. Slow wetting ameliorated this expansion by allowing dissipation of entrapped air pressures.

Experiment 2

Intracrystalline expansion accounted for a significant portion of the expansion by Ca- and Al-montmorillonite and to a lesser extent by Na-, Ca- and Al-vermiculite following saturated vapor-wetting. It was suggested that diffuse double layer formation would be inhibited during vapor-wetting due to the difference in entropy of liquid and gaseous water. The relaxation of bent and twisted crystals was also implicated as contributing to expansion during vapor-wetting. Scanning electron micrographs revealed crystal distortions diminished in the order: Na-MT > Ca-MT > Al-MT > Na-VR ≃ Ca-VR ≃ Al-VR, corresponding to the observed order of ratios of vapor-wet expansion to vapor adsorption.

Subsequent submersion of the vapor-wet clays resulted in large increases in water adsorption and expansion. Intracrystalline expansion could not contribute to these increases since it should have been complete after vapor-wetting. Furthermore, the volume of predicted osmotic adsorption was greatly exceeded by measured expansion. It was postulated that the increased expansion during liquid-phase wetting resulted largely from rotational and translational movements of crystals and groups of crystals perhaps induced by double layer repulsion to some degree, as well as by entrapped air pressures, and crystal strain relaxation. Accordingly, the increase in expansion after submersion decreased with increasing counterion valence and with increasing mineral surface charge, reflecting strengthening face-to-face and edge-to-face bonds which would restrict such movements.

The expansion of freeze-dried compacted Ca-MT was found to be much larger than that of oven-dried Ca-MT compacted to a similar density.

This was attributed to greater crystal strain in the freeze-dried clay evident in scanning electron micrographs. Greater strain broadening of the (060) x-ray diffraction peak was observed for the freeze-dried clay and its mean b-dimension was found to be slightly smaller than that of the oven-dried clay. It was suggested that crystal strain relaxation is a more probable mechanism than clay-water epitaxy to explain the relationship between b-dimension and swelling that has been reported in the literature.

Experiment 3

During the initial wetting of compacted and undisturbed Poplimento samples, variations in volume change between treatments were small despite considerable differences in initial moisture content. It was inferred that decreases in pore size with increasing compaction moisture contents counteracted the effect of moisture content differences by decreasing the accommodation of microscale expansion in large voids and by increasing expansion caused by entrapped air pressures, strain relaxation and/or differential strain. In contrast, compacted Iredell samples displayed a marked inverse relationship between compaction moisture content and swelling during the first wetting. After making allowances for differences in initial moisture content, compacted Iredell samples were noted to exhibit considerably greater expansion than undisturbed clods. Thus, it appears that changes in structure accompanying air-drying and/or compaction increase the propensity for swelling of Iredell.

Differences in soil structure of Poplimento samples were still evident after the first wet-dry cycle reflected in variations in swelling caused by entrapped air pressures during the second wetting. This mechanism accounted for 59, 50, 39, and 8% of the total for undisturbed, CL, CO, and CH Poplimento samples, respectively. This sequence appears unlikely to reflect the direct, inverse relationship between entrapped air swelling and pore size predicted by the Laplace equation. Rate of water uptake and resistance to expansion were suggested as additional factors which may be involved. Even after excluding the effect of

entrapped air pressures, expansion of Poplimento clods during the second wetting varied with sample treatment, increasing directly with compaction moisture content. Predicted intracrystalline adsorption varied little with sample treatment and accounted for only 2-9% of the expansion remaining after exclusion of swelling due to entrapped air. Predicted osmotic adsorption was also essentially constant but of much larger magnitude, accounting for 93, 133, 57, and 35% of the vacuum-wet expansion of undisturbed, CL, CO, and CH clods, respectively. Apparently, much double layer development is accommodated within large voids during the wetting of CL clods. The discrepancies between measured vacuum-wet expansion and predicted expansion of CO and CH samples were attributed to crystal strain relaxation and to differential strains occurring between crystals and groups of crystals during wetting.

During the second wetting of Iredell clods, relatively small differences in expansion were attributable to variations in swelling due to entrapped air pressures, which accounted for 23, 13, 27, and 22% of the expansion of undisturbed, CL, CO and CH samples, respectively. Intracrystalline expansion in Iredell was greater than in Poplimento, but still accounted for only approximately 10% of the remaining expansion, while osmotic adsorption accounted for approximately 60%. It is suggested that relaxation of crystal distortions which arise during drying may be responsible for a significant portion of the expansion in this high montmorillonite soil.

CONCLUSIONS

Intracrystalline expansion, while of some importance in the pure mineral systems during wetting from low initial moisture contents, appeared unlikely to be of significance in soils even during wetting from unusually dry conditions. Conversely, osmotic expansion was insignificant in the pure clays but quite appreciable in the soils. These differences reflect the greater number of platelets per crystal which occurred in the pure minerals, perhaps reflecting enhanced orientation induced during sample preparation. Osmotic adsorption and resulting expansion appeared to be inhibited by vapor-phase wetting. Compaction had little effect on the magnitude of predicted osmotic or intracrystalline expansion in either the pure minerals or soils. Swelling due to entrapped air pressures, crystal strain relaxation, and differential strains during wetting, however, were quite sensitive to variations in structure induced by compaction or drying as well as to differences in rate and method of wetting.

The results emphasize that it is erroneous to consider the forces which cause water adsorption and those which cause expansion as synonomous. A great deal of water may be retained by capillarity in pores which have expanded as a result of entrapped air pressures, crystal strain relaxation, or differential strains during wetting. The repulsion of adjacent water films is not the sole and quite likely not the most important mechanism of expansion. Thus, it is unnecessary--indeed fallacious--to consider that expansion is directly related to the volume of surface-associated water. This realization and the

observation that b-dimension is affected by crystal strain, refutes the argument that surface-water epitaxy governs swelling.

The results of this study have implications to the measurement and prediction of field volume changes as well as to the management of expansive soils. Interpretation of laboratory tests of soil swelling must take into account nuances of sample preparation as well as method and rate of wetting which may greatly affect expansion. In situ control of rate of wetting or restriction of liquid phase wetting may help ameliorate swelling in certain field situations.

LITERATURE CITED

Adamson, A. W. 1976. Physical chemistry of surfaces, 3rd ed. John Wiley & Sons, NY.

Aylmore, L. A. G. 1974. Hysteresis in gas sorption isotherms. J. Colloid Interface Sci. 46:410-416.

Aylmore, L. A. G. 1977. Microporosity in montmorillonite from nitrogen and carbon dioxide sorption. Clays Clay Miner. 25:148-154.

Aylmore, L. A. G., and J. P. Quirk. 1960. Domain or turbostratic structure of clays. Nature 187:1046-1048.

Aylmore, L. A. G., and J. P. Quirk. 1962. The structural status of clay systems. Clays Clay Miner. 9:104-130.

Barclay, L., A. Harrington, and R. H. Ottewill. 1972. The measurement of forces between particles in disperse systems. Kolloid - Z.u.Z. Polymere 250:655-666.

Barclay, L. M., and R. H. Ottewill. 1970. Measurement of forces between colloidal particles. Special discussions of the Faraday Society 1:138-147.

Barshad, I. 1960. Thermodynamics of water adsorption and desorption on montmorillonite. Clays Clay Miner. 8:84-101.

Bartell, F. E., and R. M. Suggitt. 1954. Heat of wetting of copper, graphite and silica gel. J. Phys. Chem. 58:36-40.

Baver, L. D., W. H. Gardner, and W. R. Gardner. 1972. Soil physics, 4th ed. John Wiley & Sons, Inc., NY.

Blackmore, A. V., and R. D. Miller. 1961. Tactoid size and osmotic swelling in Ca-montmorillonite. Soil Sci. Soc. Am. Proc. 25:169-173.

Bolt, G. H. 1955. Analysis of the validity of the Gouy-Chapman theory of the electric double layer. J. Coll. Sci. 10:206-218.

Bolt, G. H., and R. D. Miller. 1955. Compression studies of illite suspensions. Soil Sci. Soc. Am. Proc. 19:285-288.

Bolt, G. H., and M. Peech. 1953. The application of the Gouy theory to soil-water systems. Soil Sci. Soc. Am. Proc. 17:210-213.

Bresler, E. 1972. Interacting diffuse layers in mixed mono-divalent ionic systems. Soil Sci. Soc. Am. Proc. 36:891-896.

Cebula, D. J., R. K. Thomas, S. Middleton, R. H. Ottewill, and J. W. White. 1979. Neutron diffraction from clay-water systems. Clays Clay Miner. 27:39-52.

Dakshanamurthy, V. 1979. A stress-controlled study of swelling characteristics of compacted expansive clays. Geotech. Test J. 2:57-60.

Derjaguin, B. V., and L. D. Landau. 1941. Acta physicochim. U.R.S.S. 14:635.

Eberl, D. D. 1980. Alkali cation selectivity and fixation by clay minerals. Clays Clay Miner. 28:161-172.

Eisenman, G. 1962. Cation selective glass electrodes and their mode of operation. Biophys J. 2:259-323.

El-Swaify, S. A., and D. W. Henderson. 1967. Water retention by osmotic swelling of certain colloidal clays with varying ionic composition. J. Soil Sci. 18:223-232.

Emerson, W. W. 1962a. The swelling of Ca-montmorillonite due to water adsorption. I. Water uptake in the vapour phase. J. Soil Sci. 13:31-39.

Emerson, W. W. 1962b. The swelling of Ca-montmorillonite due to water adsorption. II. Water uptake in the liquid phase. J. Soil Sci. 13:40-45.

Emerson, W. W. 1964. The slaking of soil crumbs as influenced by clay mineral composition. Aust. J. Soil Res. 2:211-217.

Graham, J. 1964. Adsorbed water on clays. J. Pure and Appl. Chem. 14:81-90.

Greene-Kelly, R. 1974. Shrinkage of clay soils: a statistical correlation with other soil properties. Geoderma 11:243-257.

Gregg, S. J., and K. S. W. Sing. 1967. Adsorption, surface area and porosity. Academic Press, NY. 371 p.

Hawkins, R. K., and P. A. Egelstaff. 1980. Interfacial water structure in montmorillonite from neutron diffraction experiments. Clays Clay Miner. 28:19-28.

Hiemenz, P. C. 1977. Principle of colloid and surface chemistry. Marcel Dekker, Inc., NY. 516 p.

Homshaw, L. G., and J. Chaussidon. 1979. Pore size distribution in water-saturated calcium montmorillonite using low temperature heat-flow calorimetry. Proc. 6th Int. Clay Conf. 1978:141-151.

Hunt, J. P. 1965. Metal ions in aqueous solutions. W. H. Benjamin, NY.

Ihler, R. K. 1955. The colloid chemistry of silica and silicates. Cornell Univ. Press, Ithaca, NY.

Israelachvili, J. N., and G. E. Adams. 1978. Measurement of forces between two mica surfaces in aqueous electrolyte solutions in the range 0-100 nm. J. Chem. Soc. Faraday Trans. I. 74:975-1001.

Kay, B. D., and P. F. Low. 1975. Heat of compression of clay-water mixtures. Clays Clay Miner. 23:266-271.

Kemper, W. D., and J. P. Quirk. 1970. Graphic presentation of a mathematical solution for interacting diffuse layers. Soil Sci. Soc. Am. Proc. 34:347-351.

Keren, R., and I. Shainberg. 1975. Water vapor isotherms and heat of immersion of Na/Ca-montmorillonite systems - I. Homoionic clay. Clays Clay Miner. 23:193-200.

Kijne, J. W. 1968. Heats of wetting of complexes between montmorillonite and alkylammonium compounds. 9th Int. Conf. Soil Sci. Trans. Int. Soc. Soil Sci. Angus and Robertson, Sydney, Australia 1:597-605.

Kijne, J. W. 1969. On the interaction of water molecules and montmorillonite surfaces. Soil Sci. Soc. Am. Proc. 33:539-543.

Kirkham, D., and W. L. Powers. 1972. Advanced soil physics. Wiley-Interscience, NY.

Kittrick, J. A. 1969a. Interlayer forces in montmorillonite and vermiculite. Soil Sci. Soc. Am. Proc. 33:217-222.

Kittrick, J. A. 1969b. Quantitative evaluation of the strong-force model for expansion and contraction of vermiculite. Soil Sci. Soc. Am. Proc. 33:222-225.

Kolaian, J. H., and P. F. Low. 1962. Thermodynamic properties of water in suspensions of montmorillonite. Proc. 9th Nat. Conf. Clays Clay Miner. 11:71-84.

Low, P. F. 1959. Discussion of physico-chemical properties of soils: ion exchange phenomena. J. Soil Mech. Found. Div. Am. Soc. Civil Eng. No. SM2 85:79-89.

Low, P. F. 1979. Nature and properties of water in montmorillonite-water systems. Soil Sci. Soc. Am. J. 43:651-658.

Low, P. F. 1980. The swelling of clay. III. Dissociation of exchangeable cations. Soil Sci. Soc. Am. J. (In press).

Low, P. F., and D. M. Anderson. 1958a. The partial specific volume of water in bentonite suspensions. Soil Sci. Soc. Am. Proc. 22:22-24.

Low, P. F., and D. M. Anderson. 1958b. Osmotic pressure equations for determining thermodynamic properties of soil water. Soil Sci. 86:251-253.

Low, P. F., and J. F. Margheim. 1979. The swelling of clay: I. Basic concepts and empirical equations. Soil Sci. Soc. Am. J. 43:473-481.

Low, P. F., I. Ravina, and J. L. White. 1970. Changes in b-dimension of Na-montmorillonite with interlayer swelling. Nature 226:445-446.

Martin, R. T. 1962. Adsorbed water on clay: a review. Clays Clay Miner. Proc. 9th Nat. Conf. 1960. 11:28-69.

McBride, M. B. 1978. Retention of Cu^{2+}, Ca^{2+}, Mg^{2+} and Mn^{2+} by amorphous alumina. Soil Sci. Soc. Am. J. 42:27-31.

McDowell, C. 1956. Interrelationship of load, volume change, and layer thicknesses of soils to behavior of engineering structures. Proc. Hwy. Rsch. Bd. 35:754-772.

Norrish, K. 1954. The swelling of montmorillonite. Disc. Faraday Soc. 19:120-134.

Norrish, K. 1972. Forces between clay particles. Proc. Int. Clay Conf., Madrid, Spain, p. 375-382.

Norrish, K., and J. A. Rausell-Colom. 1963. Low angle x-ray diffraction studies of the swelling of montmorillonite and vermiculite. Clays Clay Miner. 10:123-149.

O'Connor, G. A., and W. D. Kemper. 1969. Quasi-crystals in Na-Ca systems. Soil Sci. Soc. Am. Proc. 33:464-469.

Parker, J. C., D. F. Amos, and D. L. Kaster. 1977. An evaluation of several methods of estimating soil volume change. Soil Sci. Soc. Am. J. 41:1059-1064.

Parker, J. C., L. W. Zelazny, S. Sampath, and W. C. Harris. 1979. Critical evaluation of the extension of zero point of charge (ZPC) theory to soil systems. Soil Sci. Soc. Am. J. 43:668-674.

Quirk, J. P. 1978. Some physico-chemical aspects of soil structural stability--a review. In W. W. Emerson, R. D. Bond, and A. R. Dexter (eds.) Modification of soil structure, John Wiley & Sons, NY, p. 3-16.

Quirk, J. P., and L. A. G. Aylmore. 1960. Swelling and shrinkage of clay-water systems. Trans. 7th Int. Cong. Soil Sci., Madison, Wisc. Int. Soc. Soil Sci. 2:378-387.

Ravina, I., and P. F. Low. 1977. Change of b-dimension with swelling of montmorillonite. Clays Clay Miner. 25:201-204.

Rhoades, J. D., R. D. Ingvalson, and H. T. Stumpf. 1969. Interlayer spacings of expanded clay minerals at various swelling pressures: an x-ray diffraction technique for direct determination. Soil Sci. Soc. Am. Proc. 33:473-475.

Ring, G. W. 1965. Shrink-swell potential of soils. Hwy. Rsch. Bd. Record 119:7-21.

Roberson, H. E., A. H. Weir, and R. D. Woods. 1968. Morphology of particles in size-fractionated Na-montmorillonites. Clays Clay Miner. 16:239-247.

Rosenquist, I. Th. 1962. The influence of physico-chemical factors upon the mechanical properties of clays. Clays Clay Miner. Proc. 9th Natl. Conf. 11:12-27.

Rowell, D. L. 1963. Effect of electrolyte concentration on the swelling of oriented aggregates of montmorillonite. Soil Sci. 96:368-374.

Rowell, D. L. 1965. Influence of positive charge on the inter- and intra-crystalline swelling of oriented aggregates of Na-montmorillonite in NaCl solutions. Soil Sci. 100:340-347.

Ruiz, C. L. 1962. Osmotic interpretation of the swelling of expansive soils. Hwy. Rsch. Bd. Bull. 313:47-77.

Schafer, W. M., and M. J. Singer. 1976. Influence of physical and mineralogical properties on swelling of soils in Yolo County, California. Soil Sci. Soc. Am. J. 40:557-562.

Schmertmann, J. H. 1973. Swell sensitivity. Geotechnique 19(4):530-533.

Schofield, R. K. 1946. Ionic forces in thick films of liquid between charged surfaces. Trans. Faraday Soc. 42(B):219-225.

Shainberg, I., and W. D. Kemper. 1966. Hydration status of adsorbed cations. Soil Sci. Soc. Am. Proc. 30:707-713.

Sposito, G., and K. L. Babcock. 1966. Equilibrium theory of the kaolinite-water system at low moisture contents, with some remarks concerning adsorption hysteresis. Clays Clay Miner. Proc. 14th Nat. Conf. 26:133-147.

Stroosnyder, L., and P. Koorevaar. 1972. Air pressure within soil aggregates during quick wetting and subsequent explosion. Symp. Fund. of Soil Conditioning, Ghent, p. 1095-1106.

Tabor, P., and R. H. S. Winterton. 1968. Surface forces: direct measurement of normal and retarded van der Waals forces. Nature 219:1120-1121.

Talsma, T. 1977. A note on the shrinkage behavior of a clay paste under various loads. Aust. J. Soil Res. 15:275-277.

Terzaghi, K. 1927. Soil classification for foundation purposes. Trans. 1st Int. Cong. Soil Sci. 4:127-157.

van Olphen, H. 1963. An introduction to clay colloid chemistry. Interscience Publ. (John Wiley & Sons), NY, 301 p.

van Olphen, H. 1965. Thermodynamics of interlayer adsorption of water in clays. I. Sodium vermiculite. J. Colloid Sci. 20:822-837.

van Olphen, H. 1969. Thermodynamics of interlayer adsorption of water in clays. II. Magnesium vermiculite. Proc. 3rd Int. Clay Conf. AIPEA (Tokyo) 1:649-657.

van Olphen, H. 1975. Water in soils. In J. E. Giesking (ed.) Soil components, Vol. 2. Springer-Verlag, NY, p. 497-527.

Verwey, E. J. W., and J. Th. G. Overbeek. 1946. Long distance forces acting between colloidal particles. Trans. Faraday Soc. 42(B):117-123.

Verwey, E. J. W., and J. Th. G. Overbeek. 1948. Theory of the stability of lyophobic colloids. Elsevier Publ. Co., NY, 205 p.

Walker, G. F. 1975. Vermiculites. In J. E. Giesking (ed.) Soil components, Vol. 2. Springer-Verlag, NY, p. 155-189.

Warkentin, B. P., G. H. Bolt, and R. D. Miller. 1957. Swelling pressure of montmorillonite. Soil Sci. Soc. Am. Proc. 21:495-497.

APPENDIX

Determination of Equilibrating Solutions for Soils in Experiment 3

To estimate the concentrations of ions in solution which would be in equilibrium with the measured quantities of exchangeable ions, Gapon exchange coefficients (k_G) between all pairs of cations were assumed equal to one. That is, for an exchange reaction:

$$M^{+m}_{1/m}X + \frac{1}{n} N^{+n} \rightleftarrows N^{+n}_{1/n}X + \frac{1}{m} M^{+m} \qquad [A1]$$

where M and N are cations of valence m and n and X is an exchange site, we write the Gapon-type equilibrium equation:

$$k_G = \frac{(N^{+n}_{1/n}X)(M^{+m})^{1/m}}{(M^{+m}_{1/m}X)(N^{+n})^{1/n}} \qquad [A2]$$

or in a somewhat less cumbersome notation:

$$k_G = \frac{\gamma_N (M^{+m})^{1/m}}{\gamma_M (N^{+n})^{1/n}} \qquad [A3]$$

where the first terms on the left in the numerator and denominator are the equivalents of adsorbed ions, and the second terms are solution concentrations; e.g., moles/l.

The ionic strength (I) of the soil solutions will be given by the following, if all cations are assumed to derive from their Cl salts:

$$I = \frac{1}{2} [(Na^+) + (K^+) + 4(Ca^{2+}) + 4(Mg^{2+}) + 9(Al^{3+}) + (Cl^-)] \qquad [A4]$$

Furthermore, for electrical neutrality:

$$(Cl^-) = (Na^+) + (K^+) + 4(Ca^{2+}) + 4(Mg^{2+}) + 9(Al^{3+}) + (Cl^-)] \quad [A5]$$

Making appropriate substitutions from the several Gapon equations yields the following cubic equations for the equilibrium solution cation concentrations:

$$I = 6\left[\frac{\gamma_{Al}}{\gamma_K}\right]^3 (K^+)^3 + 3\left[\frac{\gamma_{Ca}^2 + \gamma_{Mg}^2}{\gamma_K^2}\right](K^+)^2 + \left[\frac{\gamma_{Na}}{\gamma_K} + 1\right](K^+) \quad [A6]$$

$$I = 6\left[\frac{\gamma_{Al}}{\gamma_{Na}}\right]^3 (Na^+)^3 + 3\left[\frac{\gamma_{Ca}^2 + \gamma_{Mg}^2}{\gamma_{Na}^2}\right](Na^+)^2 + \left[\frac{\gamma_K}{\gamma_{Na}} + 1\right](Na^+) \quad [A7]$$

$$I = \left[\frac{\gamma_{Al}}{\gamma_{Ca}}\right]^3 (Ca^{2+})^{3/2} + 3\left[\frac{\gamma_{Mg}^2}{\gamma_{Ca}^2} + 1\right](Ca^{2+}) + \left[\frac{\gamma_K + \gamma_{Na}}{\gamma_{Ca}}\right](Ca^{2+})^{1/2} \quad [A8]$$

$$I = \left[\frac{\gamma_{Al}}{\gamma_{Mg}}\right]^3 (Mg^{2+})^{3/2} + 3\left[\frac{\gamma_{Ca}^2}{\gamma_{Mg}^2} + 1\right](Mg^{2+}) + \left[\frac{\gamma_K + \gamma_{Na}}{\gamma_{Mg}}\right](Mg^{2+})^{1/2} \quad [A9]$$

$$I = 6(Al^{3+}) + 3\left[\frac{\gamma_{Ca}^2 + \gamma_{Mg}^2}{\gamma_{Al}^2}\right](Al^{3+})^{2/3} + \left[\frac{\gamma_K + \gamma_{Na}}{\gamma_{Al}}\right](Al^{3+})^{1/3} \quad [A10]$$

Setting I = 0.01 M and substituting in the measured quantities of exchangeable cations gives the desired ion concentrations for the equilibrating solutions:

Soil	Solution concentrations in mmoles/l					
	Na^+	K^+	Ca^{2+}	Mg^{2+}	Al^{3+}	Cl^-
Poplimento	0.9	2.0	2.0	0.4	nil	7.7
Iredell	1.0	0.8	0.8	1.9	nil	7.2

The true values of k_G for the soils may be found by substituting into Equation A3 the appropriate calculated solution concentrations and the quantities of exchangeable ions determined on samples which have been equilibrated with the above solutions by repeated washings.

The vita has been removed from the scanned document

WATER ADSORPTION, MICROSTRUCTURE AND VOLUME CHANGE BEHAVIOR OF CLAY MINERALS AND SOIL

by

John Charles Parker

(ABSTRACT)

Swelling attributable to intracrystalline water adsorption by montmorillonite (MT) and vermiculite (VR) saturated with cations which limit interlayer expansion were calculated as the product of one-half the change in interlayer spacing determined by x-ray diffraction and the difference between total surface area taken as 800 m^2/g and external crystal surface area measured by N_2 gas adsorption. Swelling directly attributable to osmotic adsorption was calculated as the product of external surface area and theoretical double layer thickness. In homoionic, monomineralic systems of Ca- and Al-MT and Na-, Ca- and Al-VR, intracrystalline expansion accounted for 60, 70, 21, 56 and 44%, respectively, of total expansion during saturated vapor-wetting and 15, 50, 4, 12 and 13% during submersion in 0.01 N electrolyte solutions. Osmotic adsorption of these systems accounted for < 10% of the expansion on submersion in all cases.

Dry, static compaction of Ca-MT resulted in an increase in expansion with increasing initial density which was not explained by changes in predicted osmotic or intracrystalline expansion.

This was attributed to expansion caused by gaseous pressures developing ahead of advancing wetting fronts. An inverse relationship was found between pore size and swelling caused by entrapped air pressures. Slow wetting ameliorated this expansion by allowing dissipation of entrapped air.

Relaxation of crystal strains during wetting was also implicated as contributing to expansion. Electron microscopy revealed crystal strain decreased in the order: Na-MT > Ca-MT > Al-MT > Na-VR ≃ Ca-VR ≃ Al-VR. Greater expansion by freeze-dried than oven-dried Ca-MT was explained by greater crystal strain observed in the former clay. Greater strain broadening of the (060) x-ray diffraction peak was observed for the freeze-dried clay and its mean b-dimension was slightly smaller than the oven-dried clay. Crystal strain relaxation is suggested to explain the relationship between b-dimension and swelling reported in the literature.

Predicted osmotic expansion for two soils was greater than in the pure clay systems and intracrystalline expansion smaller, due to a greater ratio of external to internal surface area in the soils. Osmotic adsorption accounted for 30-70% of the soil swelling during submersion in 0.01M electrolyte solutions, while intracrystalline expansion accounted for < 10%. The magnitude of swelling due to entrapped air pressures was evaluated from the difference between expansion of atmospheric pressure-wet and vacuum-wet clods. This component accounted for 10-60% of the expansion of undisturbed and compacted samples during the second cycle of wetting from the air-dry state, but did not appear to be directly related to pore size.

Changes in structure accompanying air-drying appeared to enhance expansion, especially for the high MT Iredell soil. It was suggested that this may be the result of increases in crystal strain during drying.